Pharmacological Research 68 (2013) 68–94

Contents lists available at SciVerse ScienceDirect

Pharmacological Research

journal homepage: www.elsevier.com/locate/yphrs

Invited review

Anaplastic lymphoma kinase (ALK): Structure, oncogenic activation, and pharmacological inhibition

Robert Roskoski Jr.*

Blue Ridge Institute for Medical Research, 3754 Brevard Road, Suite 116, Box 19, Horse Shoe, NC 28742, USA

ARTICLE INFO

Article history:
Received 14 November 2012
Accepted 18 November 2012

Keywords:
Crizotinib
Drug discovery
Non-small cell lung cancer
Protein kinase inhibitor
Targeted cancer therapy
Acquired drug resistance

ABSTRACT

Anaplastic lymphoma kinase was first described in 1994 as the NPM-ALK fusion protein that is expressed in the majority of anaplastic large-cell lymphomas. ALK is a receptor protein-tyrosine kinase that was more fully characterized in 1997. Physiological ALK participates in embryonic nervous system development, but its expression decreases after birth. ALK is a member of the insulin receptor superfamily and is most closely related to leukocyte tyrosine kinase (Ltk), which is a receptor protein-tyrosine kinase. Twenty different ALK-fusion proteins have been described that result from various chromosomal rearrangements, and they have been implicated in the pathogenesis of several diseases including anaplastic large-cell lymphoma, diffuse large B-cell lymphoma, and inflammatory myofibroblastic tumors. The EML4-ALK fusion protein and four other ALK-fusion proteins play a fundamental role in the development in about 5% of non-small cell lung cancers. The formation of dimers by the amino-terminal portion of the ALK fusion proteins results in the activation of the ALK protein kinase domain that plays a key role in the tumorigenic process. Downstream signaling from ALK fusion proteins involves the Ras/Raf/MEK/ERK1/2 cell proliferation module and the JAK/STAT cell survival pathway. Furthermore, nearly two dozen ALK activating mutations participate in the pathogenesis of childhood neuroblastomas along with ALK overexpression. The occurrence of oncogenic ALK, particularly in non-small cell lung cancer, has generated considerable interest and effort in developing ALK inhibitors. Currently, crizotinib has been approved by the US Food and Drug Administration for the treatment of ALK-positive non-small cell lung cancer along with an approved fluorescence *in situ* hybridization kit used for the diagnosis of the disease. The emergence of crizotinib drug resistance with a median occurrence at approximately 10 months after the initiation of therapy has stimulated the development of second-generation drugs for the treatment of non-small cell lung cancer and other disorders. About 28% of the cases of crizotinib resistance are related to nearly a dozen different mutations of ALK in the EML4-ALK fusion protein; the other cases of resistance are related to the upregulation of alternative signaling pathways or to undefined mechanisms. It is remarkable that the EML4-ALK fusion protein was discovered in 2007 and crizotinib was approved for the treatment of ALK-positive non-small cell lung cancer in 2011, which is a remarkably short timeframe in the overall scheme of drug discovery.

Contents

Abbreviations: AL, activation loop; ALCL, anaplastic large-cell lymphoma; C-spine, catalytic spine; CRC, colorectal cancer; *D*, distribution coefficient; DLBCL, diffuse large B-cell lymphoma; EGFR, epidermal growth factor receptor; HGF/SF, hepatocyte growth factor/scatter factor; IMT, inflammatory myofibroblastic tumor; IRS1, insulin receptor substrate 1; JAK, Janus activated kinase; LE, ligand efficiency; LipE, lipophilic efficiency; MW, molecular weight; NSCLC, non-small cell lung cancer; *P*, partition coefficient; PDGFR, platelet-derived growth factor receptor; PI3K, phosphatidylinositol 3-kinase; PKA, protein kinase A; PKC, protein kinase C; PLC, phospholipase C; pY, phosphotyrosine; R-spine, regulatory spine; VEGFR, vascular endothelial growth factor receptor.

* Tel.: +1 828 891 5637; fax: +1 828 890 8130.
E-mail address: rrj@brimr.org

1043-6618/$ – see front matter © 2012 Elsevier Ltd. All rights reserved.
http://dx.doi.org/10.1016/j.phrs.2012.11.007

1. Introduction

The human protein kinase family consists of 518 genes thereby making it one of the largest gene families [1]. These enzymes catalyze the following reaction:

$$MgATP^{-1} + protein{-}OH \rightarrow protein{-}OPO_3^{2-} + MgADP + H^+$$

Based upon the nature of the phosphorylated —OH group, these proteins are classified as protein-serine/threonine kinases (385 members), protein-tyrosine kinases (90 members), and tyrosine-kinase like proteins (43 members). Moreover, there are 106 protein kinase pseudogenes. Of the 90 protein-tyrosine kinases, 58 are receptor and 32 are non-receptor kinases. A small group of dual-specificity kinases including MEK1 and MEK2 catalyze the phosphorylation of both tyrosine and threonine in target proteins; dual-specificity kinases possess molecular features that place them within the protein-serine/threonine kinase family. Protein phosphorylation is the most widespread class of post-translational modification used in signal transduction. Families of protein phosphatases catalyze the dephosphorylation of proteins thus making phosphorylation-dephosphorylation an overall reversible process [2].

Protein kinases play a predominant regulatory role in nearly every aspect of cell biology [1]. They regulate apoptosis, cell cycle progression, cytoskeletal rearrangement, differentiation, development, the immune response, nervous system function, and transcription. Moreover, dysregulation of protein kinases occurs in a variety of diseases including cancer, diabetes, and autoimmune, cardiovascular, inflammatory, and nervous disorders. Considerable effort has been expended to determine the physiological and pathological functions of protein-kinase signal transduction pathways during the past 30 years.

Besides their overall importance in signal transduction, protein kinases represent attractive drug targets. See Ref. [3] for a classification of six types of small molecule protein kinase inhibitors and Supplementary Table 1 for a list of 18 US Food and Drug Administration approved protein kinase inhibitors and Supplementary Fig. 1 for their structures. Supplementary Table 1 includes four drugs that were approved in 2012 including (a) axitinib, which is used in

the treatment of renal cell cancer, (b) bosutinib, which is used in the treatment of Philadelphia chromosome positive chronic myelogenous leukemia, (c) regorafenib, which is used in the treatment of colorectal cancer, and (d) tofacitinib (pronounced toe" fa sye' ti nib), which is used in the treatment of rheumatoid arthritis. Nine of the agents listed in the Supplementary table are multi-kinase inhibitors, and future studies will address the importance and generality of the therapeutic effectiveness of such drugs.

Supplementary material related to this article is found, in the online version, at http://dx.doi.org/10.1016/j.phrs.2012.11.007.

One characteristic property of protein kinases is that they are stringently regulated, and the mechanisms for the interconversion of dormant and active enzymes are often intricate. Taylor et al. refer to this interconversion as switching [4]. Furthermore, protein kinases have not evolved to catalyze the phosphorylation of thousands of molecules per minute like a general metabolic enzyme such as hexokinase ($k_{cat} = 6000\,min^{-1}$) [5]. When a receptor protein-tyrosine kinase is activated by its ligand, the chief phosphorylated product is the receptor itself by the process of autophosphorylation as described in Section 4.1. Thus, classical steady-state enzyme kinetics, which is based on the premise that the substrate concentration greatly exceeds that of the enzyme, fails to apply to the physiological function of protein kinases when the concentrations of the enzyme and substrate are similar. For example, Fujioka et al. measured the content of MEK and ERK in HeLa cells and found that the concentrations of these protein kinases were 1.4 μM and 0.96 μM, respectively [6]. ERK is the only known substrate of MEK, and in this case the substrate concentration is less than that of the enzyme.

Taylor et al. argue that pre-steady-state kinetics for the phosphoryl transfer is important in the analysis of protein kinase function [4]. Grant and Adams found that the pre-steady-state phosphoryl transfer rate of PKA is significantly faster than the steady-state k_{cat} (30,000 *versus* $1200\,min^{-1}$) [7]. The rapid pre-steady-state rate of enzymes, which lasts about 20 ms for PKA, is called a burst. Such kinetics are consistent with the rapid and transient reactions that have been optimized for the specific and local phosphorylation of proteins involved in a signaling pathway. Taylor et al. suggest that pre-steady-state kinetics should be used routinely in the assessment of protein kinase signaling mechanisms [4].

2. An overview of anaplastic lymphoma kinase (ALK)

Anaplastic lymphoma kinase, which is a member of the insulin receptor protein-tyrosine kinase superfamily, is most closely related to leukocyte tyrosine kinase (Ltk) [8]. In 1994, Morris et al. and Shiota et al. characterized an unknown protein-tyrosine kinase in anaplastic large-cell lymphoma (ALCL) cell lines [9,10]. These cell lines were derived from a subtype of non-Hodgkin lymphoma. The term anaplastic refers to cells that have become dedifferentiated. About 2/3rds of anaplastic large-cell lymphomas possess a balanced chromosomal translocation in which the entire nucleophosmin (*NPM*) gene on chromosome 5 is fused to the 3′ portion of the *ALK* gene (including the entire intracellular segment with its protein kinase domain) on chromosome 2. This oncogenic ALK protein kinase is a chimeric protein created by a translocation between chromosomes (2;5)(p23;q35) that generates the NPM-ALK fusion protein. This chromosomal rearrangement results in the ectopic expression of the NPM-ALK fusion protein that has a constitutively activated ALK kinase domain; the kinase was named after the disease [9]. Moreover, an echinoderm microtubule-associated protein like 4 (EML4)-ALK oncoprotein was identified in non-small cell lung cancers [11,12]. As noted later, more than two dozen other ALK fusion proteins have been described that occur in a variety of diseases [13]. Furthermore, four groups established the primary role of ALK as a critical oncogene in the pathogenesis of neuroblastoma, an aggressive and often lethal childhood cancer [14–17]. In the case of neuroblastoma, increased ALK activity is due to overexpression of ALK or to point mutations that produce an enzyme with increased activity.

Work in 1997 demonstrated that physiological ALK consists of an 18 amino-acid-residue signal peptide, a long extracellular domain (1020 amino acid residues in humans), a 21-residue transmembrane segment, and a 561 amino acid intracellular domain (UniprotKB ID: Q9UM73) [18]. The molecular weight of unmodified ALK is about 176 kDa. As a result of N-linked glycosylation of the extracellular portion of the protein, the physiological molecular weight is about 220 kDa. The intracellular portion consists of a juxtamembrane segment, a protein kinase domain, and a carboxyterminal tail (Fig. 1). The extracellular domain contains two MAM segments, one LDLa domain, and a glycine-rich portion. Each MAM (meprin, A5 protein, and receptor protein tyrosine phosphatase μ) domain consists of about 170 amino acid residues containing four cysteines that most likely form two disulfide bridges. These domains appear to possess adhesive functions and to participate in cell–cell interactions. The LDLa (low density lipoprotein class A) domain, whose function in ALK is uncertain, is characterized by a segment that contains two or more disulfide bridges and a cluster of negatively charged residues. The function of the extracellular glycine-rich domain, which contains one stretch of eight consecutive glycine residues and two stretches of six consecutive glycine residues, is also uncertain. In *Drosophila melanogaster*, point mutations of single glycine residues in the glycine-rich segment result in non-functional ALK demonstrating the importance of this domain, at least in this species [20].

Two proteins, midkine and pleiotrophin, have been reported to be the activating ligands for mammalian ALK [21,22]. These polypeptide growth factors have a monomeric mass of about 130 kDa, and they form functional dimers. These factors, which bind to heparin, are implicated in diverse processes such as neural development, cell migration, and angiogenesis. However, Motegi et al. and Moog-Lutz et al. were unable to confirm that midkine or pleiotrophin stimulated mammalian ALK under conditions where monoclonal antibodies directed against the ALK extracellular domain were able to activate its signaling [23,24]. Thus, the identity of the physiological ligand(s) for ALK is uncertain.

Mammalian ALK is thought to play a role in the development and function of the nervous system based upon the expression of its mRNA throughout the nervous system during mouse embryogenesis [18,25,26]. Iwahara et al. observed that the intensity of ALK mRNA and protein expression in mice diminishes after birth; it reaches a minimum after three weeks of age and is thereafter maintained at low levels in the adult animal [25]. Morris et al. reported that ALK mRNA is expressed in adult human brain, small intestine, testis, prostate, and colon but not in normal human lymphoid cells, spleen, thymus, ovary, heart, placenta, lung, liver, skeletal muscle, kidney, or pancreas [9].

Bilsland et al. and Lasek et al. reported that *Alk*$^{-/-}$ deficient mice are viable and fertile without any obvious alterations [27,28]. Bilsland et al. demonstrated that such adult homozygous mice have increased basal dopaminergic signaling in the frontal cortex and hippocampus [27]. They suggested that ALK may be a target for schizophrenia and depression, which are conditions associated with dysregulated monoaminergic signaling. Lasek et al. found that ALK deficiency in mice leads to augmented ethanol consumption [28]. Their data suggest that this greater consumption may be related to increased ERK1/2 signaling in the brain. This finding implies that ALK negatively regulates ERK1/2 signaling, which is not the case in most other ALK-mediated signaling processes.

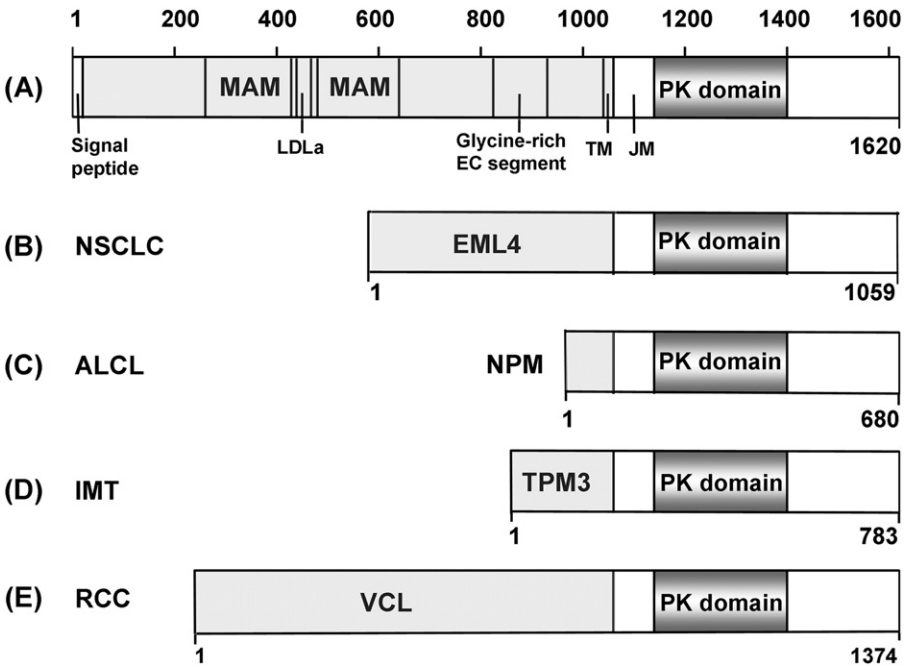

Fig. 1. (A) General structure of the native human ALK receptor protein-tyrosine kinase. The extracellular segment (residues 19–1038) of ALK contains two MAM components (264–427 and 480–626), an LDLa domain (453–471), and a glycine-rich segment (816–940). A transmembrane segment (residues1039–1059) connects the extracellular domain with the juxtamembrane segment (1060–1115) of the intracellular domain (1060–1620). The kinase domain consists of residues 1116–1392. (B)–(E) Structures of selected ALK fusion proteins that occur in the listed diseases. The numbers denote amino acid residues, and those for EML4-ALK correspond to variant 1. The entire intracellular domain (excluding the transmembrane segment) occurs in each of the fusion proteins. EC, extracellular; JM, juxtamembrane; TM, transmembrane; NSCLC, non-small cell lung cancer; ALCL, anaplastic large-cell lymphoma; IMT, inflammatory myofibroblastic tumor; RCC, renal cell carcinoma.
Adapted from Ref. [19].

3. Structure of the ALK protein kinase domain

3.1. Catalytic residues in the amino- and carboxyterminal lobes of the ALK protein kinase domain

The ALK protein kinase domain has a small amino-terminal lobe and large carboxyterminal lobe that contain several conserved α-helices and β-strands, first described by Knighton et al. for PKA [29]. The small lobe is dominated by a five-stranded antiparallel β-sheet (β1–β5) [30]. It also contains an important regulatory αC-helix that occurs in active or in quiescent positions. The small lobe contains a conserved glycine-rich (GxGxxG) ATP-phosphate-binding loop, sometimes called the P-loop, which occurs between the β1- and β2-strands (Fig. 2). The glycine-rich loop, which is the most flexible part of the small lobe, helps position the β- and γ-phosphates of ATP for catalysis. The β1- and β2-strands harbor the adenine component of ATP. The glycine-rich loop is followed by a conserved valine (V1130) that makes a hydrophobic contact with the adenine group of ATP (unless otherwise specified, all residue numbers correspond to native human ALK even when experiments were performed with ALK-fusion proteins). The β3-strand typically contains an Ala-Xxx-Lys sequence, the lysine of which (K1150) couples the α- and β-phosphates of ATP to the αC-helix. A conserved glutamate occurs near the middle of the αC-helix (E1167) in protein kinases. The presence of a salt-bridge between the β3-lysine and the αC-glutamate is a prerequisite for the formation of the activated state and corresponds to the "αC-in" conformation. The αC-in conformation is necessary but not sufficient for the expression of full kinase activity. However, the absence of this salt bridge indicates that the kinase is dormant.

The large lobe of the ALK protein kinase domain is mainly α-helical (Fig. 2) with six conserved segments (αD–αI) [30]. It also contains two short conserved β-strands (β7–β8) that contain most of the catalytic residues associated with the phosphoryl transfer from ATP to ALK substrates. The primary structure of the β-strands occurs between those of the αE- and αF-helices. The quiescent, or less active, unphosphorylated ALK protein kinase domain contains an additional helix within the activation loop (αAL [31] or αEF [32]) that immediately follows the β8-strand.

Hanks et al. identified 12 subdomains (I–VIa, VIb–XI) with conserved amino acid residue signatures that constitute the catalytic core of protein kinases [33]. Of these, the following three amino acids, which define a K/D/D (Lys/Asp/Asp) motif, illustrate the catalytic properties of ALK. An invariant β3-strand lysine (K1150) forms salt bridges with the α- and β-phosphates of ATP (Fig. 3). The catalytic loops surrounding the actual site of phosphoryl group transfer are different between the protein-serine/threonine and protein-tyrosine kinases. This loop is made up of an YRDLKPEN canonical sequence in protein serine/threonine kinases and an HRDLAARN sequence in protein-tyrosine kinases.

The occurrence of HRDIAARN in NPM-ALK, which was initially determined by Morris et al. [9], allowed them to identify ALK as a receptor protein-tyrosine kinase. The AAR sequence in the catalytic loop represents a receptor protein-tyrosine kinase signature, and RAA represents a non-receptor protein-tyrosine kinase. D1249, which is a base occurring within the catalytic loop, plays an important role in catalysis. Zhou and Adams suggested that this aspartate positions the substrate hydroxyl for an in-line nucleophilic attack [35]. See Ref. [36] for a general discussion of the enzymology of protein kinases.

The second aspartate of the K/D/D signature, D1270, is the first residue of the activation segment. The activation segment of nearly all protein kinases begins with DFG (Asp-Phe-Gly) and ends with APE (Ala-Pro-Glu). The ALK activation segment begins with DFG but it ends with PPE. Asp1270 binds Mg^{2+}, which in turn coordinates the α- β- and γ-phosphates of ATP. The primary structure of the catalytic loop of ALK, which occurs before the β7-strand, contains His1247, Arg1248, Asp1249 (Fig. 3). The primary structure of the

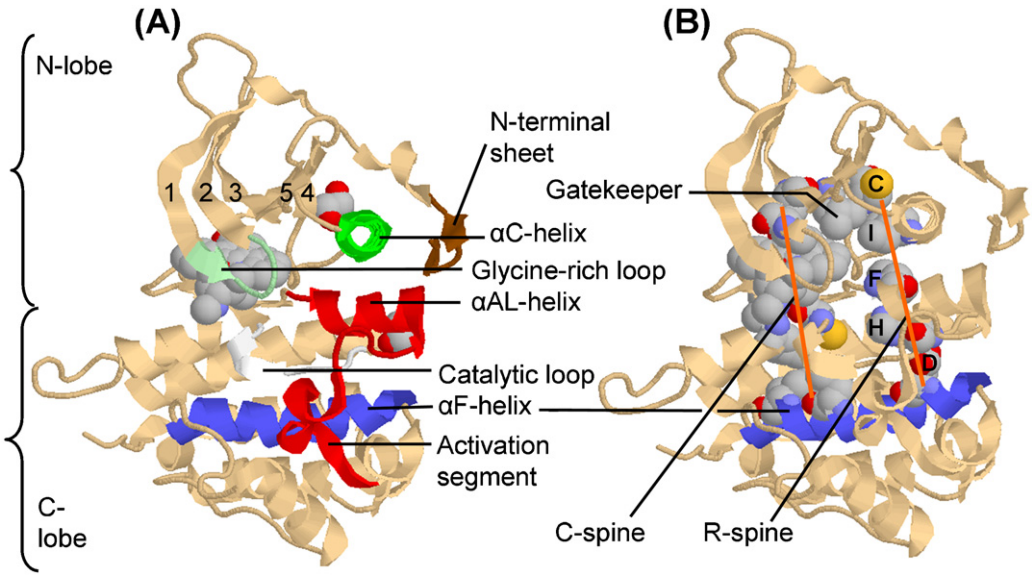

Fig. 2. (A) Ribbon diagram of human ALK. The numbers in the N-lobe label β-strands 1–5. This structure corresponds to a dormant enzyme with the activation segment blocking the peptide binding site. The αC-helix is viewed from its N-terminus. The αAL-helix occurs in the activation loop or activation segment. The space-filling model of staurosporine, an inhibitor of many protein kinases, is shown occupying the ATP-binding site beneath the glycine-rich loop, and a glycerol molecule is shown above the αC-helix and behind the αAL-helix. (B) The orange lines denote the residues (space-filling models) that constitute the catalytic and regulatory spines. Although the regulatory spine of quiescent enzymes may be broken, the structure of unphosphorylated ALK has the DFG-Asp in conformation, which is usually associated with a completed R-spine [4]. Although the isoleucine and phenylalanine of the spine are aligned, they do not contact one another as shown here. The ALK gatekeeper (Leu1196) contacts both spines. The view is the same as that of (A). Prepared from protein data bank file PDB ID: 3LCS.

activation segment occurs after that of the catalytic loop. Functionally important human ALK residues are listed in Table 1. The large lobe characteristically binds the peptide/protein substrates.

The activation segment is the most important regulatory element in protein kinases [37]. This segment influences both substrate binding and catalytic efficiency. The five-residue magnesium-positioning loop begins with the DFG of the activation segment. The middle of the activation segment, which is the most diverse part of the segment in terms of length and sequence among protein kinases, is known as the activation loop. This loop in ALK contains three phosphorylatable tyrosines. The loop is located close in the three-dimensional sense to the magnesium-binding loop, the amino-terminus of the αC-helix, and the conserved HRD component of the catalytic loop. The interaction of these three components is hydrophobic in nature, which is indicated by the double arrows in Fig. 3. Negatively charged phosphate in the activation loop of active protein kinases serves as an organizer for the active site and for the P+1 binding site.

The phosphorylation site of the peptide/protein substrate is numbered 0 (zero), the residue immediately after the phosphorylation site is P+1, and the residue immediately before the phosphorylation site is P−1. The P+1 binding site of protein kinases helps determine the substrate specificity of these enzymes by selecting amino acid residues in protein substrates that fit into

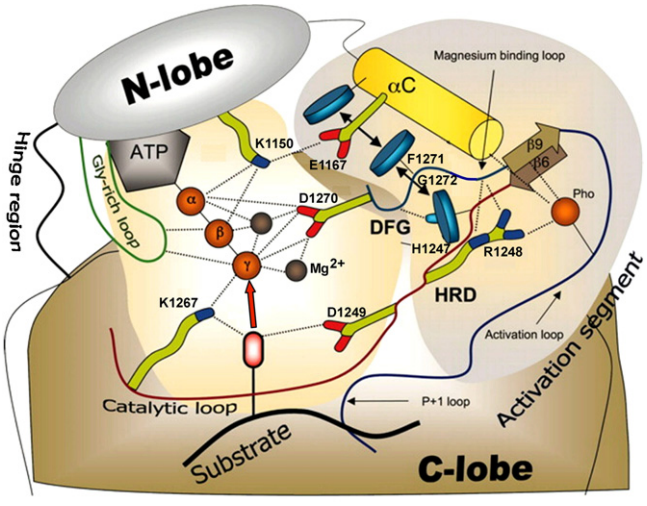

Fig. 3. Diagram of the inferred interactions between human ALK catalytic core residues, ATP, and a protein substrate. Catalytically important residues that are in contact with ATP and the protein substrate occur within the light khaki background. Secondary structures and residues that are involved in regulation of catalytic activity occur within the gray background. Hydrophobic interactions between the HRD motif (the first D of K/D/D), the DFG motif (the second D of K/D/D), and the αC-helix are shown by the double arrows while polar contacts are shown by dashed lines. Pho is the phosphate attached to Tyr1283.

This figure is adapted from Ref. [34] copyright *Proceedings of the National Academy of Sciences USA*.

Table 1
Important residues in human ALK and c-Met.

	ALK	c-Met
Protein kinase domain	1116–1392	1078–1345
Glycine-rich loop	1123–1128 GHGAFG	1085–1090 GFGHFG
The K of K/D/D, or the β3-lysine	1150	1110
αC-glutamate	1167	1127
Hinge residues	1197–1201	1159–1163
Gatekeeper residue	L1196	P1158
Catalytic HRD, the first D of K/D/D	1247–1249	1202–1204
Catalytic loop lysine	1267	1215
Activation segment DFG, the second D of K/D/D	1270–1272	1222–1224
Activation segment tyrosine phosphorylation sites	1278, 1282, 1283	1230, 1234, 1235
End of the activation segment	1297–1299 PPE	1251–1253 ALE
No. of residues	1620	1390
Molecular weight (kDa)	176.4	155.5
UniProtKB ID	Q9UM73	P08581

Table 2
Human ALK and c-Met and murine PKA residues that form the R-spine and C-spine.

	ALK	c-Met	PKA[a]
Regulatory spine			
β4-Strand (N-lobe)	Cys1182	Leu1157	Leu106
C-helix (N-lobe)	Ile1171	Met1131	Leu95
Activation loop (C-lobe) F (Phe) of DFG	Phe1271	Phe1223	Phe185
Catalytic loop His or Tyr (C-lobe)[b]	His1247	His1202	Tyr164
F-helix (C-lobe)	Asp1311	Asp1254	Asp220
Catalytic spine			
β2-Strand (N-lobe)	Val1130	Val1092	Val57
β3-AXK motif (N-lobe)	Ala1148	Ala1108	Ala70
β7-Strand (C-lobe)	Leu1256	Met1211	Leu173
β7-Strand (C-lobe)	Cys1255	Cys1210	Leu172
β7-Strand (C-lobe)	Leu1257	Leu1212	Ile174
D-helix (C-lobe)	Leu1204	Leu1165	Met128
F-helix (C-lobe)	Leu1318	Leu1272	Leu227
F-helix (C-lobe)	Ile1322	Leu1276	Met231

[a] From Ref. [34].
[b] Part of the His-Arg-Asp (HRD) or Tyr-Arg-Asp (YRD) catalytic segment sequence.

this site. The P+1 site is generally composed of the last eight residues of the activation loop.

3.2. ALK hydrophobic spines

Taylor and Kornev [30] and Kornev et al. [34] analyzed the structures of active and less active conformations of some two dozen protein kinases and determined functionally important residues by a local spatial pattern (LSP) alignment algorithm. This analysis revealed a skeleton of four non-consecutive hydrophobic residues that constitute a regulatory or R-spine and eight hydrophobic residues that constitute a catalytic or C-spine. Each spine consists of residues derived from both the small and large lobes. The regulatory spine contains residues from the αC-helix and the activation loop, whose conformations are important in defining active and less active states. The catalytic spine governs catalysis by directing ATP binding. The two spines dictate the positioning of the protein substrate (R-spine) and ATP (C-spine) so that catalysis results. The proper alignment of the spines is necessary but not sufficient for the assembly of an active kinase.

The ALK regulatory spine consists of a residue from the beginning of the β4-strand (Cys1182), from the C-terminal end of the αC-helix (Ile1171), the phenylalanine of the activation segment DFG (Phe1271), along with the HRD-histidine (His1247) of the catalytic loop. Ile1171 and comparable residues from other protein kinases are four residues C-terminal to the conserved αC-glutamate. The backbone of His1247 is anchored to the αF-helix by a hydrogen bond to a conserved aspartate residue (Asp1311). The P+1 loop, the activation loop, and the αH–αI loop bind to the αF-helix by hydrophobic bonds [34]. Table 2 lists the residues of the spines in human ALK and the catalytic subunit of murine PKA and Fig. 2B shows the location of the catalytic and regulatory spines of ALK.

The catalytic spine of protein kinases consists of residues from the amino-terminal and carboxyterminal lobes that is completed by the adenine base of ATP [30]. This spine mediates catalysis by directing ATP localization thereby accounting for the term catalytic. The two residues of the small lobe of the ALK protein kinase domain that bind to the adenine component of ATP include Val1130 from the beginning of the β2-strand and Ala1148 from the conserved Ala-Xxx-Lys of the β3-strand. Moreover, Leu1256 from the middle of the β7-strand binds to the adenine base in the active enzyme. Cys1255 and Leu1257, hydrophobic residues that flank Leu1256, bind to Leu1204 at the beginning of the D-helix. The D-helix Leu1204 residue binds to Leu1318 and Ile1322 in the αF-helix.

Note that both spines are anchored to the αF-helix, which is a very hydrophobic component of the enzyme that is entirely within the protein and not exposed to the solvent. The αF-helix serves as a sacrum that supports the spines, which in turn support the protein kinase catalytic muscle. In contrast to the protein kinase amino acid signatures such as DFG or HRD, the residues that constitute the spine were not identified by sequence analyses *per se*. Rather, they were identified by their three-dimensional location based upon a comparison of the X-ray crystallographic structures of some twenty protein kinases in their active and latent states [4,30,34,37].

Besides the hydrophobic interactions with the adenine group, the exocyclic 6-amino nitrogen of ATP characteristically forms a hydrogen bond with a backbone residue in the hinge region that connects the N- and C-lobes of the protein kinase domain. The residues in the ALK hinge include Glu1197, Leu1198, Met1199, Ala1200, and Gly1201. Most small-molecule inhibitors of protein kinases that compete with ATP binding also make hydrogen bonds with the backbone residues of the hinge region [38].

3.3. Structure of quiescent ALK protein kinase

Lee et al. and Bossi et al. were the first to determine the X-ray structure of the protein kinase catalytic domain of ALK, which was in its quiescent and unphosphorylated form [31,32]. Because ALK is a member of the insulin receptor superfamily and the X-ray structures of the quiescent and active protein kinase catalytic domain of the insulin receptor had been determined [39,40], both groups compared their structure of quiescent ALK with that of the insulin receptor protein kinase domain [31,32]. Although the conformation of activated protein kinase activation segments is similar, Huse and Kuriyan reported that the X-ray crystal structure of each quiescent enzyme usually reveals its own distinctive less active activation segment conformation [41]. These authors noted that protein kinases usually assume their less active conformation in the basal or non-stimulated state, and the acquisition of their activity may involve several layers of regulatory control [41]. Taylor et al. refer to the process of going from the latent to active conformation (and *vice versa*) as a dynamic switch [4]. As mentioned in Section 3.1, the two main regulatory elements within the catalytic domain include the αC-helix within the small lobe and the activation loop within the large lobe.

Less active unphosphorylated ALK does not possess all of the negative regulatory structural elements that the less active insulin receptor bears. First of all, dormant ALK assumes the DFG-aspartate in conformation [31,32], which corresponds to the active state, rather than the quiescent DFG-aspartate out conformation. Moreover, the dormant ALK activation loop does not obstruct the ATP-binding site as is observed in the case of the dormant insulin receptor kinase domain. The relative interlobe closure between the small and large lobes of ALK is intermediate between that of the less active open and more active closed conformations exhibited by the insulin receptor protein kinase domain. In dormant ALK, the αC-helix is rotated into the active site, properly positioning Glu1167 with Lys1150 of the β3-strand. The structurally important Lys-Glu salt bridge, which occurs in active protein kinase conformations, is observed in the unphosphorylated quiescent ALK structure.

The αC-helix, which is sequestered by (a) the αAL-helix, (b) the last two strands of the amino-terminal β-sheet (β-4 and β-5), and (c) the amino-terminal β-turn that is contributed by the juxtamembrane segment, is thus restricted in its mobility. As noted later, mutation of Lys1062 in the juxtamembrane segment results in ALK activation [14], and this observation suggests that the immobilization of the αC-helix by the juxtamembrane segment plays an important role in maintaining ALK kinase in its latent state. The distal residues of the activation loop (Cys1288-Ala1289-Met1290)

are in a position to block peptide substrate binding, thereby contributing to the latent status of the enzyme. The restricted mobility of the αC-helix, suboptimal lobe closure, and the obstruction of the peptide-binding site by the distal activation loop all contribute to enzyme dormancy.

The X-ray structures of the unphosphorylated and quiescent ALK protein kinase domain provide considerable information about its fundamental properties [31,32]. However, it would be most helpful to have the structure of the phosphorylated and active enzyme for comparison.

3.4. Steady-state enzyme kinetic parameters of quiescent and active ALK

Bresler et al. compared the enzyme kinetic parameters of the unphosphorylated and dormant ALK protein kinase catalytic domain with that of the trisphosphorylated catalytic domain [42]. They used the recombinant enzyme, ATP, and a peptide with the sequence corresponding to the activation loop of ALK for their measurements. They found that the k_{cat} for the active enzyme is about 46 fold that of the dormant enzyme (424 *versus* 9.32 min^{-1}). The K_m values for ATP were about the same for each enzyme form, but the K_m value of the peptide for the activated enzyme was reduced to about 62% of that of the unphosphorylated enzyme (1.80 *versus* 2.88 mM). These data would account for less than a two-fold activation. It is thus likely that the protein kinase activation is due to an increase in the rate of transfer of the phosphoryl group during catalysis (which was not directly measured by these workers). Note that the k_{cat}, or turnover number, of activated ALK (424 min^{-1}) is less than that of PKA (1200 min^{-1}) [7]. It would be worthwhile to determine whether there is a pre-steady-state burst of activity similar to that observed for PKA [4,7].

4. ALK phosphorylation, activation, and downstream signaling

4.1. ALK phosphorylation and activation

Our knowledge of the mechanism of activation of the complete mammalian ALK protein-tyrosine kinase is incomplete. Because ALK is highly expressed only in the nervous system during embryogenesis, it is difficult to perform experiments that address its mechanism of activation. Moreover, the identity of its activating ligands is uncertain [23,24]. More information is available for the regulation of ALK in *Drosophila melanogaster* and *Caenorhabditis elegans* [43], but it is unclear how this relates to mammals. The activating ligand in *Drosophila melanogaster* is Jeb (jelly belly), and this has no ortholog in mammals. The activating ligand in *C. elegans* is Hen-1 (hesitation 1), which also lacks a mammalian ortholog. Lemmon and Schlessinger have described the mechanism of activation of several receptor protein-tyrosine kinases [8], and this provides us with a provisional scheme for ALK activation.

Ligand binding to the extracellular domain usually activates receptor protein-tyrosine kinases by inducing receptor dimerization or oligomerization (we will assume that the dimer is the form that can be activated even though it may be the oligomer). However, the insulin receptor and the insulin-like growth factor receptor already exist on the cell surface as disulfide-linked $(\alpha\beta)_2$ dimers. Whether the less active state is monomeric or dimeric, receptor activation requires the bound ligand to induce or stabilize a specific conformation of individual receptor molecules with respect to each other to form an active complex. As described above, the ALK kinase domain is autoinhibited in *cis* by the juxtamembrane domain clamping the αC-helix in a quiescent state and by the activation loop blocking peptide substrate binding.

The probable mechanism for the ligand and dimer-induced activation of ALK involves the transphosphorylation of one activation loop tyrosine by the partner ALK protein kinase followed by the transphosphorylation of the other two activation loop tyrosines. The trisphosphorylated kinase may then catalyze the transphosphorylation of the partner ALK activation loop tyrosines. In the case of the insulin receptor, phosphorylation of Tyr1162 is followed by that of Tyr1158 and then Tyr1163 [44]. For the NPM-ALK fusion protein, it appears that Tyr1278 is phosphorylated first and that of Tyr1282 and Tyr1283 occur later (human native ALK residue numbers) [45]. Whether or not this is the order followed in the native ALK receptor is unknown and deserves study. In the case of the insulin receptor, activation loop trisphosphorylation allows the αC-helix to relax into its active state.

A possible mechanism for ligand and dimer-induced activation of ALK involves the phosphorylation of one or more of the juxtamembrane tyrosine residues (Tyr 1078, 1092, 1096, and 1131). Such phosphorylation would allow the αC-helix to assume its active state. This would be followed by the phosphorylation of the activation loop tyrosine residues. The juxtamembrane segment of Kit is autoinhibitory [46]. After stem cell factor-induced dimerization, transphosphorylation of two tyrosine residues (568 and 570) in the juxtamembrane segment occurs thus relieving its inhibition. This is followed by transphosphorylation of Tyr823 in the activation loop to yield the fully active form of Kit.

Additional experimentation is required to determine the order of ALK activation loop and juxtamembrane segment phosphorylation or to establish yet other possible activation mechanisms. One characteristic in the activation of all protein kinases with multiple phosphorylation sites is that phosphorylation follows a defined sequence and is invariant.

4.2. ALK signaling

ALK fusion proteins activate many different pathways that are interconnected and overlapping [47]. These include the Ras/Raf/MEK/ERK1/2 pathway, the JAK/STAT (Janus activated kinase/signal transducer and activator of transcription) pathway, the PI3K (phosphatidylinositol 3-kinase)/Akt (PKB) pathway, and the PLC (phospholipase C)-γ pathway. The PLC-γ and Ras/ERK1/2 pathways participate in cell proliferation, and the JAK/STAT and PI3K/Akt pathways mediate cell survival (Fig. 4).

Akt, which is also known as protein kinase B (PKB), is a protein-serine/threonine kinase that binds phosphatidylinositol bisphosphate or trisphosphate with high affinity [48]. Phosphoinositide-dependent protein kinase 1 (PDK1) and mammalian target of rapamycin complex 2 (mTORC2) catalyze the phosphorylation of Akt Thr308 and Ser473, respectively, and the bisphosphorylated and activated Akt catalyzes the phosphorylation and activation of mTOR (mammalian target of rapamycin). mTOR is also a protein-serine/threonine kinase that has dozens of substrates and participates in many cellular processes including that of cell survival. Singh et al. reported that sonic hedgehog pathway signaling is downstream of Akt in ALK-positive ALCL Karpus-299 cells [49].

Following ALK activation, additional residues not mentioned in Section 4.2 become phosphorylated. These include tyrosines 1507, 1584, 1586 and 1604 in the carboxyterminal tail, and tyrosine 1139, 1358, 1385, and 1401 in the tyrosine kinase domain [43]. It is likely that protein kinases other than ALK catalyze some of these reactions. Some of these residues serve as docking sites that bind molecules that participate in ALK-mediated signal transduction. The protein-tyrosine kinase Src interacts with oncogenic ALK, and it may participate in some of these phosphorylation reactions.

Studies of NPM-ALK have identified pTyr1096 as the binding site for insulin receptor substrate 1 (IRS1); pTyr1507 is the binding

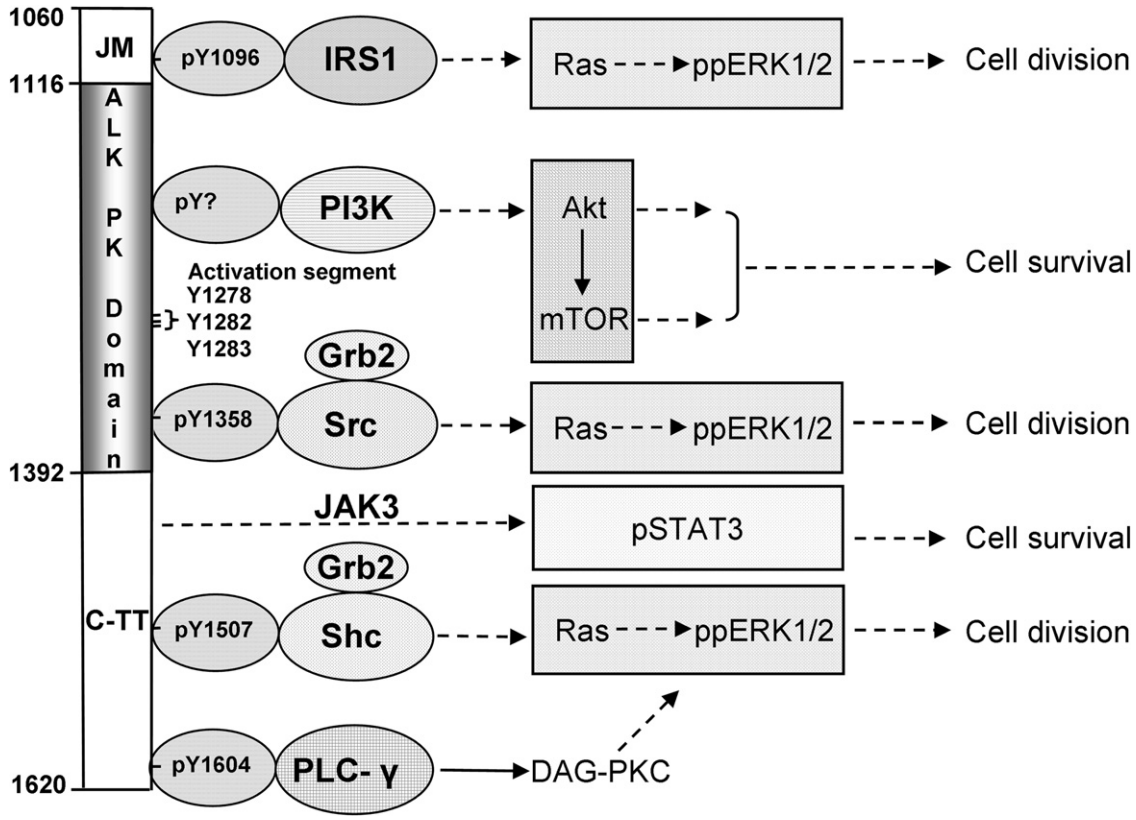

Fig. 4. ALK fusion-protein signaling pathways. Selected phosphotyrosine (pY) residues, their interacting proteins, and the relative location of the activation segment phosphorylation sites are indicated on residues corresponding to the intracellular portion of physiological ALK, which have their counterpart in the ALK fusion proteins. The numbers correspond to native human ALK amino acid residues even though most experiments on ALK signal transduction have been performed with the NPM-ALK fusion protein. The broken arrows indicate that several steps are involved in the signaling process. Diacylglycerol (DAG) activates protein kinase C (PKC). C-TT, C-terminal tail; JM, juxtamembrane; mTOR, mammalian target of rapamycin; PK, protein kinase; ppERK, bisphosphoERK; pSTAT3, phosphorylated STAT3.

site for Shc and pTyr1604 is the binding site for PLC-γ [43] (native human ALK receptor residue numbers are given; subtract 940 to obtain the NPM-ALK residue). Furthermore, Grb2 interacts with the protein-tyrosine kinase Src, which binds to pTyr1358. Grb2 also binds to Shc. IRS1, Shc, PLC-γ, Grb2, and Src are upstream of the growth-promoting Ras/ERK1/2 pathway (Fig. 4) [47]. It is unclear whether ALK catalyzes the phosphorylation of STAT3 directly or whether it activates JAK3, which then mediates STAT3 phosphorylation. Similarly, the site of interaction of ALK and PI3K has not been established.

The activation of the ERK1/2 MAP kinase pathway by NPM-ALK is intricate. Marzec et al. demonstrated that the depletion of ERK1 or ERK2 separately or together impairs cell proliferation, whereas ERK1 but not ERK2 depletion increases the apoptotic cell rate in the Karpus-299 ALK-positive cell line [50]. Apparently IRS1 and Shc do not play an essential role in the activation of the ERK1/2 MAP kinase pathway. Thus, Fujimoto et al. reported that the interaction of NPM-ALK with IRS1 and Shc is not required for cellular transformation and oncogenesis because NPM-ALK mutants unable to interact with Shc and IRS1 are still able to transform rat fibroblast NIH 3T3 cells [51]. A further complicating factor in deciphering the mechanism of signaling is that mouse ALK lacks the tyrosine residue corresponding to human ALK 1604 [43].

The JAK/STAT pathway is an important downstream signaling module of NPM-ALK [43]. Zhang et al. demonstrated that NPM-ALK induces the continuous cellular activation of STAT3 [52]. Activation of STAT3 requires its phosphorylation on a tyrosine residue that is catalyzed by a receptor or by a member of the activated JAK protein-tyrosine kinase enzyme family. Galkin et al. reported that the ALK inhibitor TEA-684 decreases STAT3 phosphorylation in Karpus-299, SU-DHL-1, and murine Ba/F3 cells, each cell line of which expressed NPM-ALK [53]. Zhang et al. demonstrated that STAT3 is phosphorylated and activated in Karpus-299 cells, and they demonstrated by immunoprecipitation that NPM-ALK and STAT3 form a complex. The nature of the binding site was not determined. Thus, STAT3 is activated by ALK either directly or indirectly through JAK3 [47].

The PLC-γ pathway is downstream from NPM–ALK and participates in the activation of the Ras/ERK1/2 MAP kinase pathway as noted above. Following its activation, PLC-γ catalyzes the hydrolysis of phosphatidylinositol bisphosphate to form inositol trisphosphate and diacylglycerol [47]. Inositol trisphosphate increases the release of Ca^{2+} from the endoplasmic reticulum and diacylglycerol activates the protein-serine/threonine kinase C (PKC). One of the downstream effectors of PKC is the Raf/MEK/ERK1/2 pathway leading to cell proliferation in a process that bypasses Ras [3]. Most studies of mammalian ALK signal transduction have been performed with oncogenic ALK, and little is known about physiological ALK signal transduction in mammals, a subject that warrants further study.

5. ALK in disease: fusion proteins, mutants, and overexpression

5.1. Anaplastic large-cell lymphoma

Stein et al. first described anaplastic large cell lymphoma in 1985 as a neoplasm of large anaplastic (bizarre) cells with abundant cytoplasm that possessed the Ki-1 antigen [54]. This antigen was identified by a monoclonal antibody that was raised against a Hodgkin disease-derived cell line. Lymphomas are neoplastic

disorders of lymphoid cells and tissues that are characterized by discrete tissue masses (tumors). On the other hand, leukemias are characterized by the presence of large numbers of neoplastic cells in the peripheral blood ($\approx 10^5$ per mm^3 or more). Within the broad group of lymphomas, Hodgkin lymphoma is segregated from all other forms (non-Hodgkin lymphomas) owing to its distinctive clinical course and response to therapy.

Anaplastic large-cell lymphoma (ALCL) is a type of non-Hodgkin lymphoma involving T-cells [55]. There is a male predominance in the adult form of the disease with a male/female ratio of about 1.5. This was the first disorder associated with an ALK fusion protein, namely NPM-ALK, and it is from this disease the enzyme received its name. Note that at least eight other fusion proteins in ALCL have been described (Table 3). Anaplastic large-cell lymphomas occur both within and outside of lymph nodes. They typically present at a late stage and are often associated with systemic symptoms. The disorder is characterized by the presence of so-called hallmark cells and CD30. Hallmark cells are of medium size and feature abundant cytoplasm, kidney-shaped nuclei, and a paranuclear eosinophilic region. CD30 is a cell membrane protein of the tumor necrosis factor receptor family. Greater than 90% of cases of ALCL contain a clonal rearrangement of the T-cell receptor.

Anaplastic large-cell lymphomas are currently treated with a combination of drugs known by the CHOP acronym [55]. CHOP consists of (a) cyclophosphamide, an alkylating agent that damages DNA by binding to it and causing cross-links, (b) hydroxydaunorubicin (also called doxorubicin, or adriamycin), an intercalating agent which inserts itself between DNA bases, (c) oncovin (vincristine), which inhibits cell duplication by binding to tubulin, and (d) prednisone or prednisolone, which are corticosteroids that are lympholytic. Localized primary cutaneous anaplastic large-cell lymphomas are treated with radiation, surgical excision, or a combination of both. Systemic ALK-positive ALCLs have a 5-year survival of 70–80%, while systemic ALK-negative ALCLs have a 5-year survival of 15–45%. The prognosis for primary cutaneous ALCL is good if there is not extensive involvement regardless of whether or not they are ALK-positive with an approximate 5-year survival rate of 90%. Although classical chemotherapeutic regimes are effective in the treatment of ALK-positive ALCL, there is significant room for improvement. NPM-ALK downstream signaling includes phospholipase C-γ, phosphatidylinositol 3-kinase, the Ras/ERK1/2 module, and the JAK/STAT pathway [43].

5.2. Non-small cell lung cancer

Lung cancer is the leading cause of cancer-related deaths worldwide with a five-year survival rate of about 15% [92]. Most lung cancers arise from a bronchus and are thus bronchogenic in nature. Lung carcinomas are classified clinically into two major groups: small-cell lung cancer (SCLC), which accounts for 10–15% of all lung cancers, and non-small cell lung cancer (NSCLC), which accounts for 85–90% of lung cancers. These disorders exhibit different responses to treatment. Surgery is the treatment of choice for NSCLC, which is less sensitive to chemotherapy and radiation than SCLC. SCLC responds relatively well to chemotherapy and radiation, but it usually has metastasized widely by the time of diagnosis thus making surgery ineffective. About 5% of non-small cell lung cancers harbor an EML4-ALK fusion protein (Table 4). All 13 fusion variants of EML4-ALK contain exons 20–29 of *ALK* (which encode the entire intracellular segment of ALK) and eight different *EML4* exons (2, 6, 13, 14, 15, 17, 18, and 20) [93]. Downstream signaling of this group of fusion proteins includes Ras/ERK1/2, Akt, and JAK/STAT [94].

The most common types of NSCLC include adenocarcinoma (≈45% of all lung cancers), squamous cell carcinoma (≈35%), and large cell carcinoma (≈10%) [92]. Adenocarcinoma of the lung (from the Greek *aden* meaning gland), which is the most common type of lung cancer in lifelong non-smokers, is characterized histologically by glandular differentiation and mucin-containing cells. Squamous cell carcinoma of the lung (from the Latin *squamosa* meaning scaly), which is more common in men than women, is characterized histologically by keratinization in the form of markedly eosinophilic dense cytoplasm and is closely correlated with a history of tobacco smoking. Squamous cell carcinoma most often arises centrally in larger bronchi. While it often metastasizes to hilar lymph nodes early in its course, it generally disseminates outside of the thorax somewhat later than other types of lung cancer. Large-cell lung carcinoma (LCLC) is a heterogeneous group of undifferentiated malignant neoplasms originating from transformed epithelial cells in the lung. These cells have large nuclei, prominent nucleoli, and a moderate amount of cytoplasm. Adenocarcinoma is usually found in the lung periphery, and small cell and squamous cell lung carcinoma are usually found centrally. Small cell lung cancers are characterized histologically by epithelial cells that are small with scant cytoplasm, ill-defined cell borders, and finely granular nuclear chromatin. ALK-positive lung cancers are most often adenocarcinomas.

The mainstay of non-metastatic lung cancer treatment is surgical removal [92]. Unfortunately, only a small proportion of lung cancers are diagnosed before the spread of the tumor from its original site, or metastasis, has occurred. In metastatic cases, combined radiotherapy and chemotherapy improves survival. Common chemotherapeutic regimes include paclitaxel and carboplatin [95]. Paclitaxel stabilizes microtubules and thus interferes with their breakdown during cell division. Carboplatin is a platinum-based anti-neoplastic agent that interferes with DNA repair. The angiogenesis inhibitor bevacizumab (Avastin®, a monoclonal antibody that binds to vascular endothelial growth factor), in combination with paclitaxel and carboplatin, improves the survival of people with advanced non-small cell lung carcinoma. However, bevacizumab increases the risk of pulmonary hemorrhaging, particularly in people with squamous cell carcinoma.

In recent years, various molecular targeted therapies have been developed for the treatment of advanced lung cancer [96]. Erlotinib (Tarceva®) is an EGFR (epidermal growth factor receptor) tyrosine kinase inhibitor that increases survival in non-small cell lung cancer and was approved by the US Food and Drug administration in 2004 for second-line treatment of advanced NSCLC. Erlotinib is most effective in treating females, Asians, nonsmokers, and those with bronchioloalveolar carcinoma, particularly those with activating EGFR mutations. Bronchioloalveolar lung cancer originates more peripherally in the lungs (close to the alveoli) and is a form of adenocarcinoma. Gefitinib (Iressa®) is another EGFR inhibitor used in the treatment of lung cancer, but it has been withdrawn from the US market owing to its failure to prolong life. However, it continues to be prescribed to those individuals who have had a good response. Based upon an overall five-year survival of about 15%, there is clearly a need for alternative therapies, especially for those with metastatic disease at the time of diagnosis. Although the proportion of NSCLCs with the EML4-ALK fusion proteins is low, the large number of total cases is large. Thus, the total number of cases of NSCLC amenable to treatment with ALK inhibitors is greater than that for all other known ALK-related cancers combined (Table 4).

5.3. Diffuse large B-cell lymphoma

Diffuse large B-cell lymphoma (DLBCL) is a malignancy of B cells, a type of leukocyte that is responsible for antibody production [97]. It is the most common type of non-Hodgkin lymphoma diagnosed in adults and accounts for 30–40% of newly diagnosed lymphomas in the United States, or 21,000–28,000 cases per year. This malignancy occurs primarily in older individuals with a median age at diagnosis of about 70 years, although it also occurs rarely in children

Table 3
Recurrent chromosomal translocations and fusion proteins involving the ALK gene in human cancers.[a]

Disease	Chromosomal abnormalities	Fusion protein (kDa)	Frequency (%)	ALK IHC[b] localization	Refs.
ALCL	t(2;5)(p23;q35)	NPM-ALK (80)	75–80	Cyto/nuclear	[9,10]
ALCL	t(2;17)(p23;q25)	ALO17-ALK (ND); two variants	<1	Cyto	[56]
ALCL	t(2;3)(p23;q21)	TFG-ALK (113); three variants	2	Cyto	[57,58]
ALCL	t(2;X)(p32;q11–12)	MSN-ALK (125)	<1	Cyto	[59,60]
ALCL	t(1;2)(q25;p23)	TPM3-ALK (104)	12–18	Cyto	[61,62]
ALCL	t(2;19)(p23;p13)	TPM4-ALK (95)	<1	Cyto	[63]
ALCL	inv(2)(p23;q35)	ATIC-ALK (96)	2	Cyto	[64–66]
ALCL	t(2;22)(p23;q11.2)	MYH9-ALK (220)	<1	Cyto	[67]
ALCL	t(2;17)(p23;q23)	CLTC1-ALK (250)	2	Cyto	[68]
NSCLC	inv(2)(p21;p23)	EML4-ALK (120); 13 variants	2–5	Cyto	[11,12]
NSCLC	t(2;3)(p23;q21)	TFG-ALK (113)	2	Cyto	[12]
NSCLC	t(2;10)(p23;p11)	KIF5B-ALK (ND)	<1	Cyto	[69,70]
NSCLC	t(2;14)(p23;q32)	KLC1-ALK (ND)	<5	Cyto	[71]
NSCLC	t(2;9)(p23;q31)	PTPN3-ALK (ND)	ND	Cyto	[72]
IMT	t(1;2)(q25;p23)	TPM3-ALK (104)	50	Cyto	[73]
IMT	t(2;19)(p23;p13)	TPM4-ALK (95)	<5	Cyto	[73]
IMT	t(2;17)(p23;q23)	CTLC-ALK (250)	<5	Cyto	[74,75]
IMT	inv(2)(p23;q35)	ATIC-ALK (96)	<5	Cyto	[76]
IMT	t(2;11;2) (p23;p15;q31)	CARS-ALK (ND)	<5	Cyto	[56,77]
IMT	t(2;2)(p23;q13) inv(2)(p23;p15;q31)	RANBP2-ALK (ND)	<5	N/M	[78,79]
IMT	t(2;4)(p23;q21)	SEC31L1-ALK (ND)	<5	Cyto	[80]
DLBCL	t(2;5)(p23;q35)	NPM-ALK (80)	ND	Cyto/nuclear	[81,82]
DLBCL	t(2;17)(p23;q23)	CLTC1-ALK (250)	ND	Granular cyto	[83]
DLBCL	t(2;5)(p23.1;q35.3)	SQSTM1-ALK (ND)	ND	Cyto	[84]
DLBCL	ins(4)(2;4)(?;q21) t(2;4)(p24;q21)	SEC31A-ALK (ND)	ND	Cyto	[85,86]
BC	inv(2)(p21;p23)	EML4-ALK (120)	<5	Cyto	[87]
CRC	inv(2)(p21;p23)	EML4-ALK (120)	<5	Cyto	[87]
CRC	t(2;2)(p23.3)	C2orf44-ALK (ND)	ND	Cyto	[88]
ESCC	t(2;19)(p23;p13)	TPM4-ALK (110)	ND	Cyto	[89,90]
RCC	t(2;10)(p23;q22)	VCL-ALK (117)	ND	Cyto	[91]

[a] Adapted from Ref. [13]. Cyto, cytoplasm; ND, not determined; N/M, nuclear/membrane; ALCL, anaplastic large cell lymphoma, DLBCL, diffuse large B-cell lymphoma; IMT, inflammatory myofibroblastic tumor; NSCLC, non-small cell lung cancer; BC, breast cancer; CRC, colorectal cancer; ESCC, esophageal squamous cell cancer; RCC, renal cell cancer.
[b] IHC, immunohistochemical.

and young adults. These aggressive tumors can arise virtually anywhere, and the first sign of this illness is typically the observation of a rapidly growing mass, sometimes with associated fever, weight loss, and night sweats. These neoplasms are characterized histologically by a relatively large cell size (five times the diameter of a small lymphocyte), a vesicular nucleus, and abundant cytoplasm that may be pale or basophilic.

A small portion of these lymphomas possess the NPM-ALK fusion protein or another fusion protein (Table 3). Diffuse large B-cell lymphomas are aggressive if untreated [97]. The traditional therapy involves the four drugs that make up the CHOP protocol, outlined in Section 5.1, along with rituximab. Rituximab is a chimeric monoclonal antibody against CD20, which is a protein found primarily on the surface of B cells [98]. Complete remission is achieved in 60–80% of cases, and about 50% of all patients remain free from disease for several years. Thus, there is room for improvement in the treatment of this disorder. Not surprisingly, those with limited disease fare better than those with widespread disease or a large bulky tumor mass.

5.4. Inflammatory myofibroblastic tumors

These rare mesenchymal neoplasms occur in soft tissues usually during the first two decades of life (Table 4) [99]. About half of these tumors possess the TPM3-ALK fusion protein (Table 3). Armstrong et al. reported that TPM3-ALK downstream signaling involves STAT3 [100]. Inflammatory myofibroblastic tumors typically arise in the lung, retroperitoneum, abdomen, or pelvis. These myofibroblastic tumors within a collagenous stroma contain an inflammatory filtrate consisting of plasma cells, lymphocytes, and eosinophils. These tumors are treated by surgical excision, but local recurrence may occur after surgery with a low risk of distant metastasis. One post-surgery chemotherapeutic regime consisted

Table 4
Constitutive ALK signaling in human cancers owing to translocations, mutations, or overexpression.[a]

Disease	Cohort	Estimated new cases in the USA per year	Comments
Non-small cell lung cancer (NSCLC)	Adults	5% of 226,000 or ≈11,300/year	Most commonly EML4-ALK fusion protein; 1% incidence in current cigarette smokers and 99% in never or former smokers
Anaplastic large cell lymphoma (ALCL)	Adults	50% of all adult ALCL are ALK-positive or ≈160/year	NPM-ALK fusion protein (80%) or other fusion protein (20%)
Anaplastic large cell lymphoma (ALCL)	Children	90% of all pediatric ALCL are ALK-positive or ≈120/year	NPM-ALK fusion protein (80%) or other fusion protein (20%)
Inflammatory myofibroblastic tumor (IMT)	Teenagers	≈75/year	TMP3/4-ALK (50%) or other fusion protein (50%)
Sporadic neuroblastoma (NBL)	Children	10% of 630/year or ≈63/year	ALK somatic point mutations or ALK amplification
Hereditary neuroblastoma (NBL)	Children	≈20/year	ALK germline point mutations

[a] www.fda.gov/downloads/advisorycommittees/committeesmeetingmaterials/drugs/oncologicdrugsadvisorycommittee/ucm236391.pdf (dated November 2010).

of cisplatin, doxorubicin (a DNA intercalator), and mitomycin C (a DNA crosslinker) [99].

5.5. Neuroblastoma

Neuroblastoma is the most common extracranial solid cancer in childhood and the most common cancer in infancy, with an annual incidence of about six hundred and fifty cases per year in the United States (Table 4). Nearly half of all neuroblastoma cases occur in children younger than two years with the median age at diagnosis of 17 months [101]. It is a neuroendocrine tumor, arising from any neural crest element of the sympathetic nervous system. It most frequently originates in the adrenal medulla, but it can also develop in nerve tissues in the neck, chest, abdomen (including the organ of Zuckerkandl located at the aortic bifurcation), or pelvis. Neuroblastoma is very unusual because it is one of the few human malignancies that can undergo spontaneous regression from an undifferentiated state to a completely benign cellular appearance.

The clinical presentation is highly variable ranging from a tumor that causes no illness to a mass that causes critical illness [101]. Signs and symptoms depend on the tumor location and metastases, if present. Moreover, the first signs of neuroblastoma are often vague thereby making diagnosis difficult. Diminished activity, decreased food intake, and fever are common signs. Classic neuroblastomas consist of small, primitive-appearing cells with dark nuclei, scant cytoplasm, and poorly defined cell borders growing in solid sheets.

Mossé et al. reported that activating mutations in the protein-tyrosine kinase domain of ALK occur in most cases of hereditary neuroblastoma [17]. Moreover, about 10% of the cases of sporadic neuroblastoma are characterized by the possession of ALK missense mutations located in the protein kinase domain [101]. Table 5 provides a list of various activating missense mutations that occur in both hereditary and sporadic neuroblastoma. Carén et al. reported that *ALK* gene amplification also occurs in neuroblastoma [103]. Del Grosso et al. found that signal transduction by amplified ALK in neuroblastoma cells involves Akt, ERK1/2, and STAT3 [104]. About 20% of neuroblastoma patients possess a high level of N-Myc amplification at chromosome 2p24, which is associated with a poorer prognosis [101].

Neuroblastoma is a disease exhibiting extreme heterogeneity, and Maris stratified it into four risk categories: very low, low, intermediate, and high risk [101]. Very low and low-risk disease can frequently be cured with surgery alone. Intermediate-risk disease is treated with surgery and chemotherapy. High-risk neuroblastoma is treated with surgery, radiation, bone marrow/hematopoietic stem cell transplantation, biological-based therapy with 13-*cis*-retinoic acid (which can induce terminal differentiation in neuroblastoma cell lines), and with intensive chemotherapy. The latter include cisplatin (a DNA crosslinker), etoposide (a topoisomerase inhibitor), vincristine (a microtubule-disrupting agent), doxorubicin (a DNA intercalator), and cyclophosphamide (a DNA alkylator). With current treatments, people with very low, low, and intermediate risk disease have an excellent prognosis with cure rates of above 85% for very low risk, greater than 75–85% for low risk, and 50–75% for intermediate risk disease. In contrast, therapy for high-risk neuroblastoma in the past two decades resulted in cures of less than 50%. There is considerable room for improvement in the treatment of intermediate and high-risk neuroblastoma.

5.6. Anaplastic thyroid cancer

Thyroid cancer is the most common malignant disease involving an endocrine gland [105]. The vast majority of thyroid cancers, including anaplastic thyroid carcinomas, are tumors of the thyroid follicular epithelium. Anaplastic thyroid carcinomas are one of the most aggressive solid tumors, with a median survival of about 3–5 months after diagnosis [106]. Death results from local growth and consequent compromise of vital structures in the neck [107]. These tumors account for 2% of all thyroid cancers [105], but anaplastic thyroid carcinomas contribute to 14–50% of overall thyroid cancer mortality [106]. People with this disease present at an older age (median, 65 years) than those with other types of thyroid cancers. Nearly half of these individuals have a history of differentiated thyroid cancer, and this finding is consistent with the notion that anaplastic thyroid carcinoma develops by dedifferentiation of existing tumors. Histologically, these tumors contain dedifferentiated giant cells, spindle cells with a sarcomatous appearance, or both types of cells.

Unlike most thyroid carcinomas, anaplastic thyroid cancer is usually unresectable owing to its high propensity for invading surrounding tissues, and it is resistant to other treatment modalities [105]. Palliative treatment consists of radiation therapy, chemotherapy with doxorubicin, or both. Murugan and Xing reported that about 10% of patient samples and cell lines derived from anaplastic thyroid cancer exhibit mutations in the *ALK* gene (Table 5) [102]. The incidence of new cases of thyroid cancer in the US is about 56,000 and the annual number of deaths is about 1800 (www.cancer.gov/cancertopics/types/thyroid). If 2% of the total number of cases are anaplastic in nature [107] (1130/year) and if 10% possess a mutation in ALK [102], the total number of thyroid cancers with ALK mutations is about 110/year. Thus, about 6% of thyroid cancer deaths may be associated with an ALK missense mutation. There is considerable room for improvement in the treatment of anaplastic thyroid cancer, and targeting tumors with ALK mutations represents an important step in producing better clinical outcomes.

5.7. Rhabdomyosarcoma

Sarcomas (from the Greek *sarx* meaning flesh) are cancers that arise from transformed cells of mesenchymal origin including skeletal muscle. Sarcomas, which are rare, make up less than 1% of all adult solid malignant tumors and about 20% of all pediatric solid malignant cancers [108]. Although many types of sarcomas are benign, rhabdomyosarcoma (a skeletal muscle neoplasm) is almost always malignant. Rhabdomyosarcoma is the most common soft tissue sarcoma of childhood and adolescence and usually appears before age 20. These tumors are classified histologically as embryonal, alveolar, and pleomorphic. The rhabdomyoblast, which is present in each of these subtypes, contains eosinophilic granular cytoplasm rich in thin and thick muscle filaments. The term alveolar comes from the microscopic appearance. The tumor cells seem to be arranged in the same pattern as the cells of the small air sacks, or alveoli, in the lungs. However, this is a structural and not actual similarity. Embryonal rhabdomyosarcomas account for 2/3rds of all cases, which is followed by the alveolar and then the rare pleomorphic subtype.

Rhabdomyosarcoma occurs most commonly in the head, neck, bladder, arms, legs, and trunk [109]. Rhabdomyosarcoma is treated with surgery, radiotherapy, and chemotherapy. Several drugs are used in the treatment of rhabdomyosarcoma including actinomycin D (an RNA synthesis inhibitor), cyclophosphamide, doxorubicin, irinotecan (a DNA topoisomerase inhibitor), and vincristine. Persons with rhabdomyosarcoma have a five-year survival rate of 50–85%.

van Gaal et al. reported that ALK protein is highly expressed in alveolar rhabdomyosarcoma and less so in the embryonal subtype (81% *versus* 32%, respectively) [110]. Moreover, elevated *ALK* gene copy number occurs in both the alveolar (88%) and embryonal subtypes (52%). Increased ALK expression was found in all metastatic tumors but in only 1/3rd of the tumors without

Table 5
Missense ALK mutations in human cancers.

Disease	Mutation	Comment	Refs.
Neuroblastoma	Lys1062Met	Lys1062 occurs in the juxtamembrane segment, which may be inhibitory. Mutations in this segment may relieve its inhibitory action	[14]
Neuroblastoma	Thr1087Ile	Thr1087 occurs in the juxtamembrane segment. See Lys1062Met	[14]
Neuroblastoma	Asp1091Asn	Asp1091 occurs in the juxtamembrane segment. See Lys1062Met	[15,17]
Neuroblastoma	Gly1128Ala	Gly1128 occurs in the glycine-rich loop, and this mutation may make it easier for ATP to gain access to its binding site	[17,32]
Neuroblastoma	Thr1151Met	Thr1151, which is next to catalytic Lys1150, forms an H-bond with Glu1129 in the β1–β2 loop adjacent to the ATP-binding site, and this mutation may make it easier for ATP to gain access to its binding site	[15,32]
Neuroblastoma	Met1166Arg	Met1166 occurs in the αC helix and forms part of a hydrophobic core with αC, αAL, and the N-terminal β-turn. Its mutation may destabilize its interactions with the αAL-helix and N-terminal β-turn thereby allowing the αC-helix to assume a more active position	[17]
Neuroblastoma	Ile1171Asn	Ile1171 is an R-spine residue that occurs in the αC-helix and forms part of a hydrophobic core with the αAL-helix. Its mutation to Asn may promote the formation of an H-bond with the backbone carbonyl of Val1180 which would help stabilize the R-spine and facilitate activation	[17,32]
Neuroblastoma	Phe1174Cys	Phe1174 is at the C-terminal end of the αC-helix. Phe1174 packs with Phe1271 (F) of the DFG motif and Phe1245 distal to the αE-helix in the inactive enzyme, which are part of a hydrophobic core. Mutation of Phe1174 may relax the steric clash with Phe1245 allowing the latter to assume its active position	[14,16,32]
Neuroblastoma	Phe1174Ile	See Phe1174Cys	[17]
Neuroblastoma	Phe1174Leu	See Phe1174Cys	[14–17]
Neuroblastoma	Phe1174Val	See Phe1174Cys	[14,16]
Neuroblastoma	Arg1192Pro	Arg1192 is on the β5-strand and forms a salt bridge with Glu1161 of the αC-helix, which helps to hold the αC-helix away from the C-lobe. Its mutation to Pro eliminates this interaction and may allow the αC-helix to assume a more active position	[17,32]
Neuroblastoma	Ala1234Thr	Ala1234 occurs in the αE-helix and contacts the αI-helix, but it is unclear how its mutation activates ALK	[15]
Neuroblastoma	Phe1245Cys	Phe1245 occurs in the catalytic loop and forms part of a hydrophobic core with the αC- and αAL-helix and the N-terminal β-turn. Mutation of Phe1245 may eliminate its interaction with Phe1174 just distal to the αC-helix thereby allowing the enzyme to assume a more active conformation	[15,17,32]
Neuroblastoma	Phe1245Leu	See Phe1245Cys	[14]
Neuroblastoma	Phe1245Val	See Phe1245Cys	[15,17]
Neuroblastoma	Ile1250Thr	Ile1250 occurs immediately after the HRD of the catalytic loop, and its side chain abuts against the HRD His1247. The mutation of Ile1250 to Thr may influence the activation segment properties thereby leading to enhanced activity	[17,32]
Neuroblastoma	Arg1275Gln	Arg1275 occurs in the αAL-helix and is in contact with the αC-helix. Its mutation may allow the αC-helix and the activation segment to assume more active positions	[14–17,32]
Neuroblastoma	Arg1275Leu	See Arg1275Gln	[16]
Neuroblastoma	Tyr1278Ser	Tyr1278 occurs within the activation loop just distal to the αAL-helix and is in contact with the N-terminal β-turn. These regions restrict the mobility of the αC-helix, and mutation of Tyr1278 may allow the αC-helix to assume a more active position	[16,32]
Anaplastic thyroid cancer	Leu1198Phe	Leu1198 is in the hinge region between the small and large lobes, and this mutation may allow more optimal interlobe closure or it may make it easier for ATP to gain access to its binding site	[102]
Anaplastic thyroid cancer	Gly1201Glu	Gly1201 is in the hinge region between the small and large lobes. See Leu1198Phe	[102]

metastasis. Furthermore, ALK expression is correlated with a poor prognosis. These investigators suggest that ALK may play a role in rhabdomyosarcoma biology and may provide a potential therapeutic target for these tumors.

6. Oncogenic activation of ALK

6.1. ALK activation following chromosomal translocations or inversions with the formation of ALK fusion proteins

Since the initial discovery of the NPM-ALK fusion protein in human anaplastic lymphoma cell lines [9], more than two dozen different ALK fusion proteins have been described in various malignancies including breast, colorectal, esophageal squamous cell, non-small cell lung and renal cell carcinomas and in diffuse large B-cell lymphomas and inflammatory myofibroblastic tumors (Table 3). The prevalence of the ALK fusion proteins in these malignancies is generally low, which thereby limits their usefulness as drug targets. Despite the occurrence of the EML4-ALK fusion protein in only about 5% in non-small cell lung cancers, the large number of cases of this disease makes this the most prevalent disease target for ALK kinase inhibitors. Although more than half of the cases of anaplastic large-cell lymphomas possess the NPM-ALK fusion protein, this is a rare malignancy so that the total incidence of new cases is small (Table 4).

The transcription of the fusion protein is driven by the promoter of the ALK partner protein [43]. This accounts for the ectopic expression of the ALK kinase domain in various cell types; full-length ALK is ordinarily expressed in large amounts only in the developing nervous system. The cellular localization of the ALK fusion proteins is determined by the fusion partner. The fusion partner mediates the ligand-independent dimerization of the ALK-fusion protein, and dimerization leads to activation of the protein kinase domain as described in Section 4.1. Dimerization thus produces oncogenic activation. The physiological function of the fusion partners and the inferred mechanism of dimerization are provided in Table 6.

6.2. ALK activation by missense mutations in neuroblastomas and in anaplastic thyroid carcinomas

As noted in Section 2, four groups of investigators established the primary role of ALK missense mutations as playing a critical role in the pathogenesis of both sporadic and hereditary

Table 6
ALK-fusion partner properties.

Partner	Abbreviations[a]	Physiological function	Structure	MW[b] (kDa)	UniProtKB ID
AICAR transformylase/IMP cyclohydrolase	ATIC	Catalyzes two steps in purine biosynthesis	Unique N-terminal dimerization domain	64.6	P31939
ALK oligomerization partner on chromosome 17	ALO17	E3 ubiquitin-protein ligase	Coiled-coil dimerization domain	591	Q63HN8
Clathrin heavy chain 1	CLTC	Found in coated pits and vesicles	N-terminal β-propeller that can interact with multiple proteins	192	Q49AL0
Cysteine-tRNA synthetase	CARS	Catalyzes cysteine-tRNA formation	Forms monomers and dimerization mechanism is unknown	85.4	P49589
Echinoderm microtubule-associated protein-like 4	EML4	May participate in microtubule assembly	Contains basic and WD (Trp-Asp) repeats, but only the basic domain is essential for transforming activity [11]	102	A6H8Y6
Kinesin-1 heavy chain	KIF5B	Kinesin-motor domain participates in microtubule-based movement	Forms oligomers composed of two heavy chains and two light chains	110	P33176
Kinesin light chain 1	KLC1	Participates in microtubule-based movement	Coiled-coil N-terminus	65.3	Q07866
Moesin (membrane-organizing extension spike protein)	MSN	Binds proteins to the inner aspect of the plasma membrane	N-terminal FERM[c] domain binds to various proteins	67.8	P26038
Non-muscle myosin heavy chain	MYH9	Participates in cytokinesis	N-terminal myosin head forms protein complexes	227	P35579
Nucleophosmin	NPM	Ribosome biogenesis, protein chaperoning	Decamer formed by two pentameric rings associated in a head-to-head fashion	32.6	P06748
Highly similar to protein-tyrosine phosphatase non-receptor type 3	PTPN3	Protein-tyrosine phosphatase	N-terminal FERM[c] domain binds to various proteins	98.9	B7Z9V1
Ran-binding protein 2	RANBP2	Imports proteins into the nucleus	Contains N-terminal TPR[d] repeat that form protein–protein complexes	358	P49792
SEC31 homolog A (*S. cerevisiae*)	SEC31L1	Forms transport vesicles from the endoplasmic reticulum	Contains 7 WD repeats that form protein-protein complexes	133	O94979
Sequestosome-1	SQSTM1	Adapter protein involved in cell differentiation	N-terminal OPR[e] domain mediates homo-oligomerization	47.6	Q13501
Testis-specific Y-encoded-like protein 2	TSPYL2	Part of the CASK/TRB1/TSPYL2 transcriptional complex	Interacts with several proteins, but the mechanisms are unknown	79.4	Q9H2G4
TRK-fused gene	TFG	Unknown	Coiled-coil dimerization domain	43	Q92734
Tropomyosin α3-chain	TPM3	Binds to actin filaments	Coiled-coil dimerization domain	32.8	P06753
Tropomyosin α4-chain	TMP4	Binds to actin filaments	Coiled-coil dimerization domain	28.5	P67936
Vinculin	VCL	Actin-filament binding protein	Vinculin N-terminus forms complexes with many proteins	124	P18206
WD repeat-containing protein C2orf44	C2orf44	Unknown	Contains two N-terminal WD repeats that form protein-protein complexes	79.1	Q9H6R7

[a] The gene name is the same as the abbreviation except for ALO17, which corresponds to gene RN213 encoding E3 ubiquitin-protein ligase RNF213.
[b] Molecular weight of the full-length partner.
[c] The FERM domain is a widespread protein module involved in localizing proteins to the plasma membrane where F denotes 4.1 protein, E denotes ezrin, R denotes radixin, and M denotes moesin.
[d] The TPR (tetratricopeptide) is a 34 amino-acid-residue motif.
[e] The OPR domain (octicosapeptide repeat) is a 28 amino-acid-residue motif.

neuroblastoma [14–17]. Furthermore, Murugan and Xing identified two novel point mutations in the *ALK* gene in anaplastic thyroid carcinoma that reside in the protein kinase domain, but they found no mutations in the matched normal tissues or in well-differentiated thyroid cancers [102]. Most of the activating mutations occur within or near important regulatory regions such as the intracellular glycine-rich segment, the αC-helix, or the activation segment. Table 5 contains a list of ALK mutants along with proposed mechanisms of activation of their protein-tyrosine kinase activities.

Bresler et al. examined the enzyme steady-state kinetic parameters of the quiescent and the phosphorylated ALK kinase domain Phe1174Leu and Arg1275Gln activating mutants and compared them with the wild type quiescent and phosphorylated protein [42]. They found that phosphorylation of the wild type protein leads to a 45-fold activation when compared with the quiescent enzyme. Moreover, they found that the unphosphorylated Phe1174Met mutant had 86% of the activity of the phosphorylated wild type enzyme (365 *versus* 424 min^{-1}) (Table 7). The increased activity of the Phe1174Met mutant cannot be explained by changes in the K_m for the peptide substrate or ATP. It is most likely due to a change

Table 7
Steady-state enzyme kinetic parameters of trisphosphorylated (ppp) and unphosphorylated wild type and mutant ALK kinase domains.[a]

Wild type ALK	pppALK	ALK	pppALK/ALK fold alteration
k_{cat}	$424 \pm 63\ min^{-1}$	$9.32 \pm 0.85\ min^{-1}$	45.5
$k_{cat}/K_{m,peptide}$	$3.93 \times 10^3\ M^{-1}\ s^{-1}$	$53.8\ M^{-1}\ s^{-1}$	13.7
$k_{cat}/K_{m,ATP}$	$4.45 \times 10^4\ M^{-1}\ s^{-1}$	$1.16 \times 10^3\ M^{-1}\ s^{-1}$	38.8
$K_{m,peptide}$	1.80 ± 0.17 mM	2.88 ± 0.42 mM	0.625
$K_{m,ATP}$	134 ± 7 μM	159 ± 12 μM	1.19
Phe1174Met ALK	–	–	–
k_{cat}	$436 \pm 51\ min^{-1}$	$365 \pm 61\ min^{-1}$	1.19
$k_{cat}/K_{m,peptide}$	$5.82 \times 10^3\ M^{-1}\ s^{-1}$	$0.662 \times 10^3\ M^{-1}\ s^{-1}$	8.79
$k_{cat}/K_{m,ATP}$	$6.67 \times 10^4\ M^{-1}\ s^{-1}$	$4.79 \times 10^4\ M^{-1}\ s^{-1}$	1.39
$K_{m,peptide}$	1.25 ± 0.20 mM	9.18 ± 1.43 mM	0.136
$K_{m,ATP}$	109 ± 1 μM	127 ± 11 μM	0.858
Arg1275Gln ALK	–	–	–
k_{cat}	$347 \pm 15\ min^{-1}$	$119 \pm 63\ min^{-1}$	2.92
$k_{cat}/K_{m,peptide}$	$4.16 \times 10^3\ M^{-1}\ s^{-1}$	$0.773 \times 10^3\ M^{-1}\ s^{-1}$	5.38
$k_{cat}/K_{m,ATP}$	$2.33 \times 10^4\ M^{-1}\ s^{-1}$	$0.607 \times 10^4\ M^{-1}\ s^{-1}$	3.83
$K_{m,peptide}$	1.39 ± 0.10 mM	2.56 ± 0.32 mM	0.543
$K_{m,ATP}$	248 ± 15 μM	326 ± 33 μM	0.761

[a] Data from Ref. [42].

in the rate of phosphoryl group transfer from ATP to the peptide substrate. The activity of the Arg1275Gln mutant was 28% that of the phosphorylated wild type protein, which represents a 13-fold activation when compared with basal wild type kinase activity.

7. ALK inhibitors

7.1. Crizotinib: a combined ALK and c-Met inhibitor

7.1.1. ALK and c-Met as drug targets

The diseases outlined in Section 5 represent conditions that may be amenable to treatment with targeted ALK inhibitors. These include anaplastic large-cell lymphoma, non-small cell lung cancer, diffuse large B-cell lymphoma, inflammatory myofibroblastic tumors, neuroblastoma, anaplastic thyroid cancer, and rhabdomyosarcoma. Additional possibilities include subsets of breast, colorectal, esophageal squamous cell, and renal cell carcinomas (Table 3).

c-Met is a receptor protein-tyrosine kinase whose activating ligand is hepatocyte growth factor/scatter factor (HGF/SF) [111]. c-Met is the hepatocyte growth factor receptor (HGFR). Like ALK, c-Met was initially discovered as an oncogenic fusion protein, namely translocated promoter region (TPR)-Met [112]. The term Met originally referred to the methyl group in the carcinogen (N-methyl-N′-nitroso-guanidine) used in a human osteogenic sarcoma cell line to generate the fusion protein [112]. Under physiological conditions, c-Met promotes tissue remodeling, morphogenesis, wound repair, and organ homeostasis [111]. In addition to its role in promoting cell division and survival under both physiological and pathological conditions, c-Met also plays a role in the metastasis of cancer cells. c-Met may even be considered an acronym for "mesenchymal-epithelial transition" factor [113] or an abbreviation for "metastasis." In this review, the cellular protooncogene will be referred to as c-Met in order to distinguish it from the abbreviation for the amino acid methionine (Met).

Like ALK, c-Met consists of an extracellular ligand-binding domain, a transmembrane segment, a juxtamembrane segment, a protein kinase domain, and a carboxyterminal tail [111]. Following HGF/SF binding, protein kinase activity is activated following receptor dimerization and phosphorylation of Tyr1234 and Tyr1235 in the enzyme activation segment. Following activation, c-Met mediated phosphorylation of two tyrosine residues (Tyr1349 and Tyr1356) in the carboxyterminal tail provides binding sites for signal-transduction docking proteins including Gab1, Grb2, PLC, and Src. Several serine residues (966, 988, 990, 997, and 1000) and a threonine residue (977) in the juxtamembrane segment undergo phosphorylation (UniprotKB ID: P08581). The functional significance of these modifications is unknown. Table 1 contains a list of selected residues in the c-Met protein kinase domain that are catalytically important, and Table 2 contains a list of the residues that make up the R- and C-spines.

A large number of disorders that exhibit sustained c-Met activation owing to stimulation, overexpression, or mutations are potential c-Met inhibitor drug targets, which include lymphomas and rhabdomyosarcomas [114,115]. Activating point mutations of the c-Met protein kinase domain occur in sporadic and inherited human renal and hepatocellular carcinomas [116,117]. Moreover, activating mutations of c-Met are clonally selected for during the metastasis of head and neck cancers [118] as their frequency increased from 2% in primary tumors to 50% in the metastatic tumors. This finding indicates that aberrant c-Met is associated with tumor progression and metastasis. Moreover, it is possible that wild type c-Met may participate in the metastatic process thereby increasing the number of cancers that may be c-Met inhibitor targets. c-Met promotes angiogenesis and lymphangiogenesis [119], which participate in tumor formation and progression [120], suggesting that c-Met inhibition may play additional roles in limiting tumorigenesis.

7.1.2. Development of crizotinib

Cui et al. published a comprehensive paper describing their development of crizotinib using structure-based drug design (SBDD) [113]. These investigators monitored the progress of optimization using lipophilic efficiency (LipE) as an index of binding effectiveness, which is given by the following equations:

$$\text{LipE} = \text{p}K_\text{i} - \text{cLog } D \quad (1)$$

$$\text{LipE} = \text{pIC}_{50} - \text{cLog } D \quad (2)$$

Eq. (1) corresponds to the inhibition of the purified protein kinase domain (K_i), and Eq. (2) corresponds to the inhibition protein kinase activity in intact cells (IC_{50}). The p of pK_i or of pIC$_{50}$ is the negative of the Log_{10} of the K_i or the negative of the Log_{10} of the IC_{50}. cLog D is the calculated log of the distribution coefficient, which is the ratio of the drug solubility in octanol/water at a specified pH, usually 7.4. A related term, cLog P, is the calculated log of the partition coefficient, which represents the solubility of a molecule in octanol/water ignoring the ionizations that change as a function of pH. One of the twists of fate is that their original target was c-Met, but crizotinib was approved by the US Food and Drug Administration for the treatment of locally advanced or metastatic non-small cell lung cancers that harbor the EML4-ALK fusion protein.

Their search for a c-Met inhibitor began with 3-substituted indolin-2-ones using the structure of PHA-665752 (Fig. 5A), a competitive inhibitor, bound to the protein kinase domain of c-Met (PDB ID: 2WKM) [113]. These workers found that the activation segment of quiescent unphosphorylated c-Met forms a wedge between the small lobe five-stranded β-sheet and αC-helix that displaces the helix from its catalytically competent position, and they set out to use this unique dormant conformation as a basis for drug design. Recall from Section 3.3 that the activation segments of various dormant protein kinases have different three-dimensional structures while the segments of the active forms of protein kinases are similar. In the initial series of experiments, Cui et al. modified the indolinone group and sulfone linker and arrived at a novel 5-aryl-3-benzyloxy-2-aminopyridine scaffold (Fig. 5B) [113]. ATP, the indolinone group of PHA-665752, and 2-aminopyridine of the scaffold bind to backbone residues of the hinge region that links the small and large lobes. They stated that the 2-aminopyridine NH group makes a hydrogen bond with the backbone carbonyl group of the hinge Pro1158 residue, and the ring nitrogen makes a hydrogen bond with the backbone–NH group of the hinge Met1160 residue.

Next, Cui et al. optimized the 3-benzyloxy group that binds to the hydrophobic pocket and interacts with Tyr1230 of the c-Met activation segment [113]. After synthesizing and characterizing more than a dozen compounds, they found that the attachment of an α-methyl-2, 6-dichloro-3-fluoro-benzyloxy group to the scaffold yielded a drug with improved properties and a cellular IC_{50} of 20 nM. After studying several dozen compounds with 5-aryl substitutions of the ethoxypyridin-2-amine core, they synthesized and characterized the racemic version of crizotinib. The R-form of the compound (Fig. 5C) proved to be the most effective. Although several purified protein kinases exhibited nanomolar IC_{50} values, they found that only c-Met (8.0 nM), ALK (20 nM), and RON (80 nM) exhibited cell-based IC_{50} values of less than 100 nM [113].

Cui et al. determined the X-ray crystal structure of crizotinib bound to the kinase domain of ALK (Fig. 6A), which was not their original target [113]. Like most type I protein kinase inhibitors [3], the drug is close to the hinge residues (Leu1196, Glu1197, Leu1198, Met1199, Ala1200, and Gly1201). It also interacts with the G-rich loop Leu1122, the gatekeeper Leu1196, the C-spine

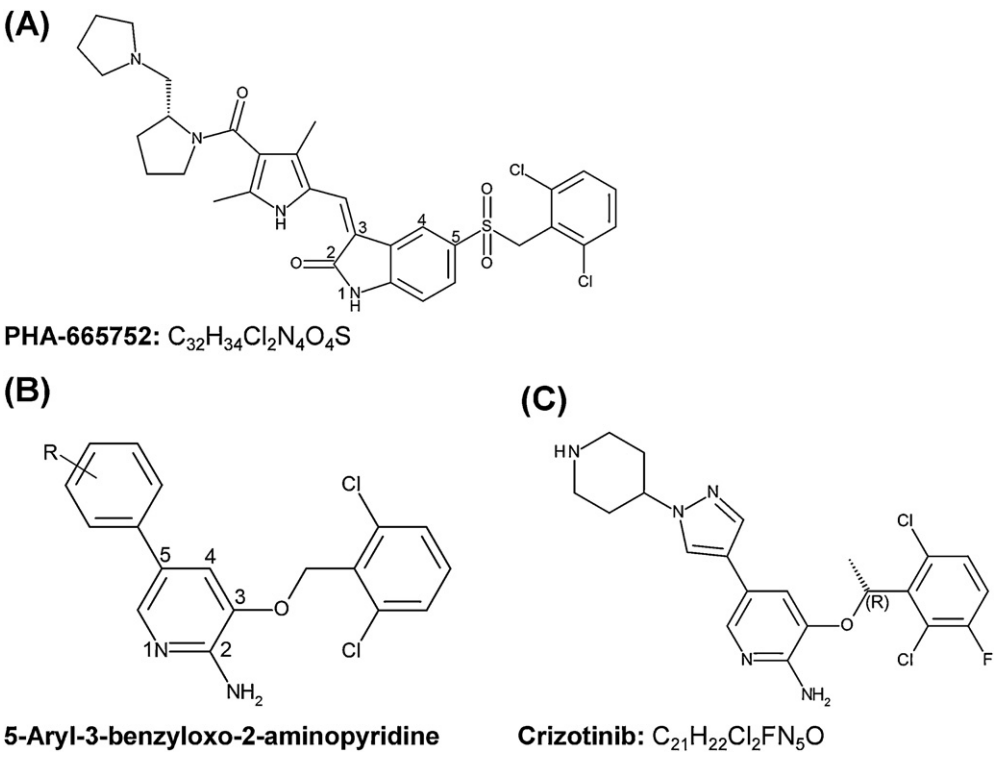

Fig. 5. Structure of crizotinib and selected lead compounds.

Val1130, Ala1148, and Leu1256 residues, and the activation segment Asp1270 (the D of DFG). Note that most of the activation segment extends away from crizotinib (Fig. 6A). Like ALK, crizotinib binds to several residues in the c-Met hinge region (Lys1161, His1162, Gly1163), to the G-rich loop Val1092, to the C-spine Met1211 and Val1092, and to the R-spine Leu1157. In contrast to ALK, the c-Met activation segment is close to crizotinib (Fig. 6B). Thus, crizotinib makes several contacts with the c-Met activation segment including Asp1222 (the D of DFG), Ala1226, and Tyr1230 (a phosphorylation site).

7.1.3. Inhibition of tumor growth and drug-induced toxicity

Human anaplastic large-cell lymphoma Karpas-299 and SU-DHL-1 cells express NPM-ALK [121]. Crizotinib inhibits the ALK-fusion protein kinase activity in these cells with an IC_{50} of 24 nM. It also inhibits the growth of these cells with IC_{50} values of 32 and 43 nM, respectively. The drug also increases the number of apoptotic cells after 24 and 48 h of treatment. In mice bearing Karpas-299 tumor xenografts (200 mm^3 initial tumor volume), oral crizotinib treatment produced complete tumor regression in 15 days [121]. Analysis of the tumors revealed that crizotinib

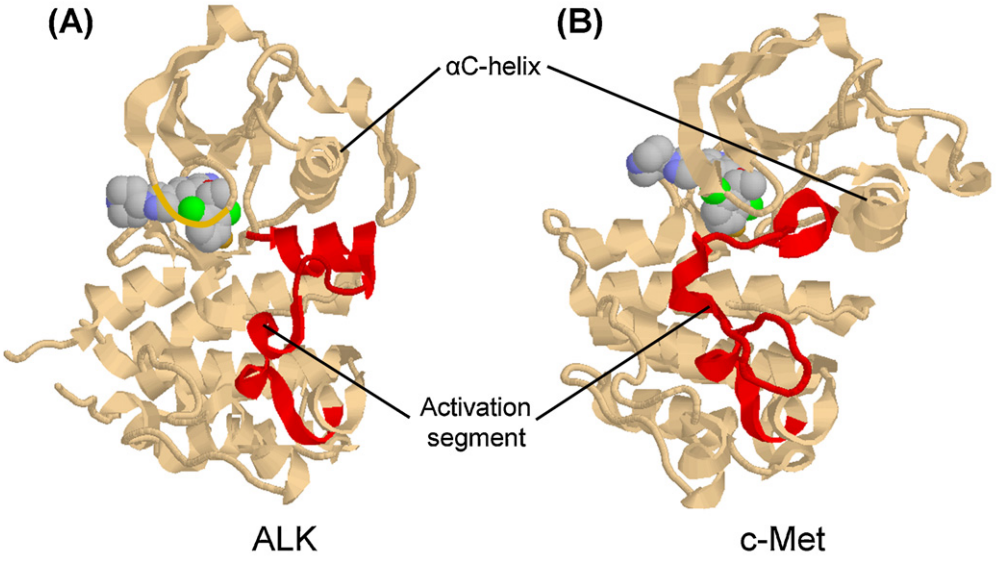

Fig. 6. Comparison of the structures of human ALK (A) and c-Met (B) with bound crizotinib (space-filling model). Note that the proximal activation segment of c-Met is close to the drug while that of ALK is not. The structure of ALK was prepared from PDB ID: 2XP2 and 3LCS (activation segment middle residues 1281–1289) and the structure of c-Met was prepared from PDB ID: 2WGJ.

reduced the levels of phosphorylated NPM-ALK, Akt, PLC-γ1, and STAT3.

People with ALK-positive NSCLC were identified using the Vysis ALK Break-Apart Fluorescence *in situ* Hybridization (FISH) Probe Kit. In one study that included 136 individuals, there was one complete response and 67 partial responses with a median duration of response of ≈42 weeks (www.accessdata.fda.gov/drugsatfda_docs/label/2012/202570s003lbl.pdf). All of these individuals had received prior systemic therapy. In another study of 82 patients (67 of whom received prior systemic therapy), crizotinib reduced tumor size in 57% of them and stabilized the disease in a further 33% [122]. Based upon these studies, the US Food and Drug Administration approved crizotinib (Xalkori®) for the treatment of locally advanced or metastatic non-small cell lung cancer that is ALK-positive as detected by the FDA-approved Vysis diagnostic kit noted above. This approval does not specify a requirement for prior therapies, and crizotinib can be used in the first-line setting. We will know in a few years how effective such first-line therapy is.

As noted in Section 2, *Alk*$^{-/-}$ deficient mice are viable and fertile without any obvious alterations [27,28]. Thus, inhibition of ALK activity *per se* should be associated with low toxicity owing to the non-essential nature of physiological ALK. Most side effects during crizotinib treatment are minimal with gastrointestinal symptoms occurring in about 50% and mild visual impairment occurring in about 40% of drug recipients [122]. However, more severe drug-induced hepatotoxicity occurred in about 5% of people during clinical trials. Camidge and Doebele reported that the hepatotoxicity was manifested by elevated serum aspartate aminotransferase and alanine aminotransferase activities [123]. They reported that other severe (grade 3 or 4) adverse side effects attributed to crizotinib include fatigue, neuropathy, neutropenia, and lymphopenia. They also reported that the rapid onset of low testosterone in men is a commonly occurring adverse event attributed to crizotininb. Of mechanistic importance is the possibility that the neuropathy and low testosterone may be related to the inhibition of physiological ALK, the mRNA of which is expressed in low levels in the human adult nervous system and in larger amounts in the human testis [9].

7.1.4. Acquired crizotinib resistance

As noted by Winer and colleagues "Biologically, the cancer cell is notoriously wily; each time we throw an obstacle in its path, it finds an alternate route that must then be blocked" [124]. Not surprisingly, crizotinib resistance occurs in people who initially benefited from treatment, and this resistance develops rapidly. For example, Katayama et al. reported that crizotinib resistance occurred in ALK-positive NSCLC patients ($N = 18$) in a range of 4–34 months with a median of 10.5 months [125]. These investigators identified mutations in the ALK protein-tyrosine kinase domain in four individuals (22%) and gene amplification in an additional case (6%) amounting to a total of 28%. At this early stage, it appears that mutations in the *ALK* fusion protein gene account for a minority of cases of acquired crizotinib drug resistance.

Katayama et al. found that alternative signaling pathways including those of the EGFR and Kit protein-tyrosine kinases were upregulated in some NSCLC samples [125]. For example, four of nine samples exhibited an increase in EGFR activation in the resistant samples when compared with the corresponding pre-treatment sensitive samples supporting a possible role of EGFR in mediating crizotinib resistance. One of these four cases had a secondary ALK mutation indicating that more than one mechanism for resistance occurs within the same tumor. They found that one patient sample of six that could be examined exhibited *Kit* gene amplification in the resistant sample when compared with the pre-treatment sensitive sample.

A crizotinib-resistant ALK protein kinase domain mutation was discovered in an early clinical trial. The Phe1174Leu mutation, which confers ALK resistance, was found in a person with an inflammatory myofibroblastic tumor who at first responded but then became refractory [126]. Although this residue occurs at the carboxyterminal end of the important regulatory αC-helix, it is not close to the crizotinib-binding site. This particular mutation is an activating mutation (Table 5), which presumably alters the tertiary structure of ALK so that crizotinib is less able to bind to the autoinhibitory conformation.

Two additional mutations (Cys1156Tyr and Leu1196Met) were found in two different clones in one person who had undergone treatment for ALK-positive NSCLC with crizotinib [127]. Leu1196 is the gatekeeper residue that occurs next to the ATP and crizotinib binding site, and gatekeeper mutations often influence type II drug binding, where type II inhibitors bind to the quiescent DFG-Asp out conformation [3]. Moreover, these mutations often involve the substitution of a larger residue such as leucine for a smaller residue such as methionine, and the larger residue blocks access to an adjacent hydrophobic pocket [128]. In the case of ALK, we have the substitution of a methionine for the larger leucine, and the basal ALK enzyme has a DFG-Asp in conformation that is the target of type I kinase inhibitors [3,31,32].

Substitution of a smaller residue indicates that the ALK Leu1196Met gatekeeper mutation does not confer crizotinib resistance by blocking access to a hydrophobic pocket. Azam et al. reported that the substitution of isoleucine or methionine for the threonine gatekeeper mutation in the Src, Abl, and PDGFRα/β, and EGFR protein kinases results in the activation of enzyme activity [129]. They reported that methionine increases activity more than isoleucine (they did not compare it with leucine). The gatekeeper residue occurs near the tip of the hydrophobic R-spine (Section 3.2) (Fig. 2B), and these investigators ascribed enzyme activation to the ability of the hydrophobic gatekeeper to strengthen the R-spine and promote formation of the active conformation of the protein.

Lovly et al. reported that the introduction of the Leu1196Met mutation into the EML4-ALK fusion protein leads to greater cellular baseline levels of phosphorylation thereby suggesting that this gatekeeper mutation leads to increased protein kinase activity [130]. Moreover, direct protein kinase activity measurements indicated that the ALK Leu1196Met mutant kinase domain is catalytically more active than the wild type enzyme (personal communication from Dr. J. Jean Cui). This raises the likelihood that the substitution of methionine for leucine destabilizes the wild type autoinhibitory conformation to which crizotinib ordinarily binds thereby conferring drug resistance. Thus, crizotinib resistance is due to enzyme activation and not to the gatekeeper blockade of an adjacent hydrophobic pocket. Additional work on the enzyme kinetic parameters of wild type ALK, the gatekeeper mutant, and other ALK mutants is warranted.

Additional mutations in samples from NSCLCs have been identified in the ALK kinase domain in people resistant to crizotinib. Some of the resistance mutations block crizotinib binding directly and others alter the structure of ALK to decrease drug binding indirectly. One mutation involves the insertion of a threonine residue after Thr1151 yielding a Thr-Thr sequence, which may lead to a decrease in the apparent K_m value for ATP [125] (Table 8). Leu1152 occurs in the β3-strand and interacts with the αC-helix; the Leu1152Arg mutation may allow the αC-helix to assume a more active position and destabilize the wild type autoinhibitory conformation to which crizotinib binds. The Cys1156Tyr mutation is distal to the αC-helix and the mechanism of conferring resistance is indirect (Table 8). The Gly1202Arg residue occurs immediately after the hinge region in the large lobe and abuts with crizotinib. Mutation to the larger arginine residue may directly impair drug binding. Asp1203, which is in direct contact with crizotinib, is on the bottom of the drug binding site. The size difference between aspartate and the mutant asparagine (Asp1203Asn) is not great, and it is

Table 8
ALK kinase mutations associated with acquired resistance to crizotinib.[a]

Mutation	ALK-fusion protein	Refs.	Inferred mechanisms of resistance
1151ThrIns	Not reported	[125]	This insertion may disrupt a critical hydrogen bond between Thr1151 and the backbone carbonyl group of Glu1129, which is next to Lys1130 (the K of K/D/D). As a consequence, this mutation may decrease the apparent K_m for ATP thereby enabling ATP to more effectively compete with and inhibit crizotinib binding
Leu1152Arg	EML4-ALK E6;A20	[132]	This residue occurs in the β3-strand and interacts with the αC-helix; this mutation may destabilize the wild type autoinhibitory conformation to which crizotinib binds
Cys1156Tyr	EML4-ALK E13;A20	[131]	Cys1156 is too far from crizotinib to block its binding, but it interacts directly with Leu1152. The tyrosine mutant may perturb Leu1152 (see above entry) and thereby destabilize the dormant enzyme conformation to which crizotinib binds
Phe1174Leu	RANBP2-ALK	[133]	Phe1174 is at the C-terminal end of the αC-helix. This activating mutation (Table 5) alters the structure of ALK so that crizotinib is less able to bind to the autoinhibitory conformation
Leu1196Met	EML4-ALK E13;A20	[125,127,130,133]	The activating gatekeeper mutation destabilizes the wild type autoinhibitory conformation to which crizotinib binds
Leu1198Pro	EML4-ALK	[134]	Leu1198 occurs immediately after the β4-strand and is above and close to crizotinib. The mutation to Pro will introduce a kink and alter the structure of the strand. A few plausible hypotheses exist that can account for drug resistance, but the precise mechanism is uncertain
Gly1202Arg	Not reported	[125]	Gly1202 occurs in the β5-αD loop and is in contact with the pyrazolyl ring of crizotinib; mutation to a larger residue may block crizotinib binding directly
Asp1203Asn	EML4-ALK	[134]	Aspartate occurs on the bottom of the crizotininb binding site. It is unclear how its mutation to asparagine would decrease the inhibitory potency of crizotinib
Ser1206Tyr	Not reported	[125]	Ser1206 occurs in the middle of the αD-helix and is about 6 Å below crizotinib; the Tyr1206 mutant may be large enough to block crizotinib binding directly
Gly1269Ala	EML4_ALK E6;A19 and EML4-ALK E6;A20	[133]	Gly1269 is in the ATP-binding pocket and contacts crizotinib; conversion to Ala may block crizotinib binding directly

[a] This table is adapted from Ref. [131]. The possible mechanisms of resistance are inferred from the X-ray structure of crizotinib bound to ALK (PDB ID: 2XP2).

unclear how this mutation might bring about crizotinib resistance. The Ser1206Tyr mutation occurs within the αD-helix, which is below the ATP/crizotinib binding site as protein kinases are usually viewed. The large tyrosine residue may block drug binding directly. The Gly1269Ala mutation occurs immediately before the DFG activation loop and is in direct contact with crizotinib. The mutation of glycine to the larger alanine may block crizotinib binding directly.

Katayama et al. experimented with NSCLC H3122 cells that express EML4-ALK and are sensitive to crizotinib [135]. They exposed the sensitive cells to increasing concentrations of crizotinib over a period of four months and generated one group of cells that they maintained in 0.6 μM crizotinib (H3122 CR0.6 cells, where CR refers to crizotinib resistant) and a second group of cells that they maintained in 1 μM crizotinib (H3122 CR cells). They found that the H3122 CR cells maintained ALK phosphorylation when grown in 1 μM crizotinib. Moreover, the downstream ALK signaling molecules, Akt and ERK, were also phosphorylated under these conditions. They found that the *EML4-ALK* gene is amplified in these cells. Besides exhibiting an increase in gene copy number per cell, these investigators found that these cells contained the ALK-resistant Leu1196Met gatekeeper mutation that was previously reported in a person with acquired resistance to crizotinib [127]. Katayama et al. found that the H3122 CR0.6 cells exhibited amplification of the *EML4-ALK* fusion protein, but none exhibit the gatekeeper mutation at Leu1196 [135]. These investigators found that treatment of both the parental H3122 and H3122 CR cell lines with siRNAs directed against ALK suppressed cell proliferation, thus indicating that ALK activity is a prerequisite for their growth.

The resistance of ALK-positive NSCLC to crizotinib can be divided into three groups. The first group is exemplified by a kinase mutation as outlined above, and the second group is resistant owing to upregulation of ALK as a result of gene amplification, or copy number gain. The third group is independent of ALK and is related to activation of other signal transduction pathways or to other mechanisms. This resembles the situation for BCR-Abl resistance to imatinib observed in the treatment of chronic myelogenous leukemia [136]. Next-generation ALK inhibitors alone may overcome resistance to mutations or copy number gain, but they are unlikely to overcome resistance to upregulation of other pathways. In the case of upregulation of EGFR or Kit, prescribing inhibitors targeting these enzymes represents a potential therapy.

7.2. CH5424842

7.2.1. CH5424842 and inhibition of the growth of cell lines and animal xenografts

Kinoshita et al. published a comprehensive paper describing their development of the ALK inhibitor CH5424802 (Chugai Pharmaceutical Co.), which is an orally effective benzo[*b*]carbazole derivative (Fig. 7A) [137]. Of some 400 protein kinases, only ALK, cyclin G-associated protein-serine/threonine kinase (GAK), and leukocyte tyrosine kinase (Ltk) exhibited biochemical IC_{50} values for CH5424802 of less than 10 nM. Sakamoto et al. reported that this compound prevents the phosphorylation of ALK in NCI-H2228 NSCLC cells expressing EML4-ALK, and it suppresses the phosphorylation of STAT3 and Akt, which are downstream ALK effectors (Fig. 4) [138]. The drug decreases the viability of these cells, but not ALK fusion protein negative cells. These investigators reported that CH5424802 induces caspase3/7, apoptotic markers, in these cells. They also found that the drug inhibits the growth of two lymphoma cell lines (Karpas-299 and SR-786) that express the NPM-ALK fusion protein, but it does not affect the growth of the HDLM-2 Hodgkin disease lymphoma cell line that does not express the fusion protein. Moreover, the drug inhibits the growth of NB-1 neuroblastoma cells that contain amplified ALK and Kelly cells that harbor the ALK Phe1174Leu activating mutation, but the drug does not inhibit the growth of the parent SK-N-Fl cell line [138].

Using mouse xenografts, Sakamoto et al. reported that CH5424802 produces growth inhibition and tumor regression of NCI-H2228 NSCLC cells expressing EML4-ALK [138]. They demonstrated that the drug decreases the phosphorylation of EML4-ALK in these tumors. It also inhibits the growth of these cells containing the Leu1196Met gatekeeper mutation that confers crizotinib resistance. However, the drug has no antitumor effect in the xenografts

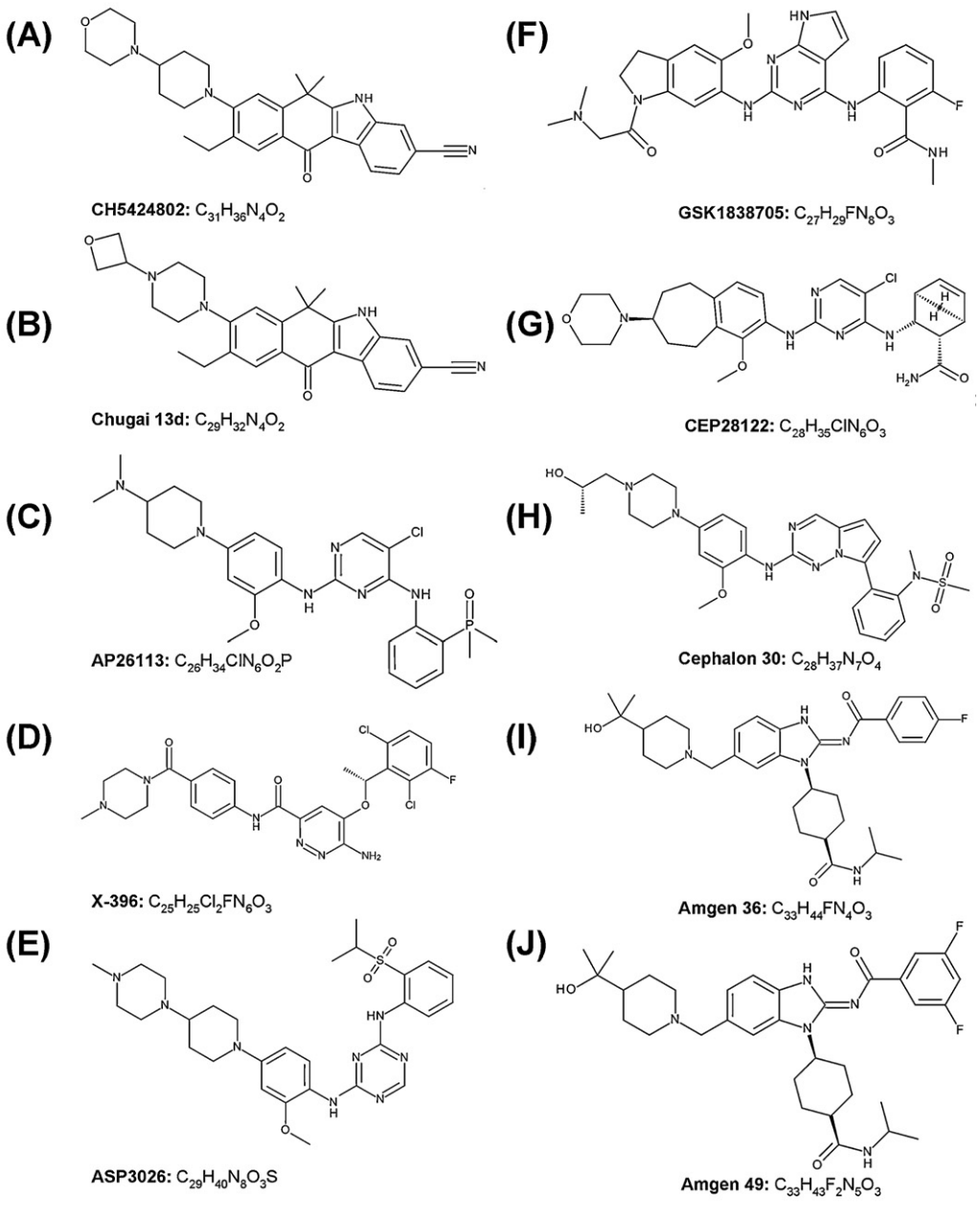

Fig. 7. Structures of selected ALK inhibitors. The left portion of each molecule most likely extends toward or into the solvent and the right portion interacts with hydrophobic regions and other sections of the ALK protein kinase domain.

of A549, which is an NSCLC line that does not express an ALK fusion protein. Sakamoto et al. also found that CH5424802 inhibits the growth of two anaplastic large-cell lymphoma cell lines (Karpas-299 and SR-786) expressing NPM-ALK, and it inhibits the growth of ALK-amplified neuroblastoma (NB-1) cells in mouse xenografts *in vivo* [138]. They also determined the oral bioavailability (71%) and half-life (8.6 h) of the drug in mice. CH5424802 is currently in stage I/II human clinical trials in Japan.

7.2.2. Structure of the ALK protein kinase domain with bound CH5424802

As in the case of crizotinib bound to the protein kinase domain of human ALK [113], Sakamoto et al. reported that CH5424802 binds to the DFG-Asp in conformation (PDB ID: 3AOX) [138]. Like crizotinib, CH5424802 is in close contact with the hinge residues. Whereas crizotinib binds to the first residue of the activation segment (the D of DFG, or Asp1270), CH5424802 makes no contact with the activation segment, which is pointed away from the drug, The carbonyl oxygen of the drug forms a hydrogen bond with the backbone NH of Met1199 of the hinge region. The benzo[*b*]carbazole group occupies the flat pocket to which the adenine base of ATP binds. The drug abuts Ala1148 and Leu1256 of the R-spine. Leu1196 in the small lobe is close to the carbon atom of the cyano group indicating an efficient CH/π interaction. These investigators suggest that the cyano group may exhibit a similar interaction with the methionine occupying this position in the Leu1196Met mutant, which may explain the effectiveness of CH5424802 as a Leu1196Met mutant inhibitor.

7.3. Chugai compound **13d**

Kinoshita et al. reported that compound **13d** (Chugai Pharmaceutical Co.), which is another orally effective benzo[*b*]carbazole derivative (Fig. 7B), is an inhibitor of ALK [139]. The compound inhibits recombinant ALK with an IC_{50} of 2.9 nM and the Karpus-299 cellular NPM-ALK with an IC_{50} of 12.9 nM. The drug inhibited insulin receptor protein-tyrosine kinase activity with an IC_{50} value of 460 nM, but it did not inhibit Kit or c-Met. These investigators also found that the drug given once daily (2, 6, or 20 mg/kg) inhibits Karpus-299 xenografts in athymic nude mice in a dose-dependent fashion in the absence of weight loss or other signs of toxicity.

7.4. AP26113

Katayama et al. reported that AP26113, which is an orally effective 2, 6-diaminopyrimidine derivative (Fig. 7C, Ariad Pharmaceuticals), inhibits ALK and EGFR protein kinase activity [135]. They found that AP26113 decreases cell growth and ALK phosphorylation and induces apoptosis in both the parental and crizotinib-resistant H3122 NSCLC (H3122 CR) cells described in Section 7.1.4. Somewhat higher concentrations of AP26113 are required to inhibit cell growth in the H3122 CR cells owing to amplification of the fusion protein gene. AP26113 inhibits growth of murine Ba/F3 pro-B cells expressing either native EML4-ALK (IC_{50} = 10 nM) or the EML4-ALK Leu1196Met mutant (IC_{50} = 24 nM). These workers found that AP26113, but not crizotinib, suppressed the growth of H3122 CR cell xenografts transplanted into athymic nude mice. AP26113 is undergoing phase I/II human clinical trials for the treatment of non-small cell lung carcinoma, anaplastic large-cell lymphoma, diffuse large B-cell lymphoma, and inflammatory myofibroblastic tumors (www.clinicaltrials.gov).

Katayama et al. found that tanespimycin (17-AAG), an inhibitor of heat shock protein 90 (Hsp90), diminishes the growth of Ba/F3 cells that expressed the native or EML4-ALK Leu1196Met mutant to a similar extent [135]. Tanespimycin decreases both the levels of phosphorylated and unphosphorylated ALK with similar potencies in the parental and resistant cells. These investigators suggested that Hsp90 inhibition represents an alternative therapeutic strategy for overcoming acquired resistance to crizotinib owing to the acquisition of a resistance mutation. Tanespimycin is undergoing or has undergone more than 50 clinical trials for a large number of disorders including EML4-ALK-positive NSCLC (www.clinicaltrials.gov).

7.5. X-396

Lovly et al. reported that X-396 is an orally effective aminopyridazine-based compound (Fig. 7D, Xcovery Inc.) that inhibits ALK and c-Met receptor protein kinase activity [130]. Based upon a competitive binding assay, they found that this drug has an IC_{50} for ALK of less than 0.4 nM when compared with crizotinib, which has an IC_{50} value of 4.5 nM. Both drugs bind to c-Met with comparable IC_{50} values of less than 1 nM. X-396 inhibits the proliferation of H3122 NSCLC cells harboring the *EML4-ALK* E13:A20 variant with an IC_{50} of 15 nM while crizotinib exhibits a value of 150 nM (E13 refers to the last exon of *EML4* that occurs in the fusion protein and A20 is the first exon from *ALK* that occurs in the fusion protein). X-396 inhibits the proliferation of SU-DHL-1 anaplastic large-cell lymphoma cells containing NPM-ALK with an IC_{50} of 9 nM while crizotinib has an IC_{50} of 73 nM. Furthermore, X-396 inhibits the growth of SY5Y neuroblastoma cells bearing the ALK Phe1174Leu mutation with an IC_{50} of 68 nM while crizotinib has a value of 338 nM. In murine Ba/F3 pro-B cells engineered to express EML4-ALK E13;A20 wild type protein (22 nM), the Leu1196Met mutant (106 nM), and the Cys1156Tyr mutant (48 nM), X-396 inhibits their growth with the indicated IC_{50} values. The IC_{50} values for crizotinib were an order of magnitude greater in each these cell lines.

Lovly et al. found that X-396 inhibits the growth of H3122 xenografts in athymic nude mice with twice daily oral administration of 25 mg/kg with the absence of weight loss or other signs of toxicity [130]. Although X-396 is unable to achieve mouse brain concentrations equivalent to those in blood plasma, it is able to moderately penetrate the blood–brain barrier. Thus X-396 achieves concentrations greater than its IC_{50} cellular inhibitory values in brain, while crizotinib fails to achieve its comparable therapeutic concentration. The ability to cross the blood–brain barrier is important because the brain is one of the chief metastatic sites for NSCLC in humans. Sometimes the first symptom of lung cancer is a seizure induced by metastatic spread to the brain.

Lovly et al. reported that X-396 was ≈10-fold more potent that crizotinib in inhibiting the growth of Ba/F3 cells expressing wild type EML4-ALK E13;A20 (IC_{50} of 22 nM for X-396 *versus* 250 nM for crizotinib) [130]. They examined the sensitivity of cells containing *EML4-ALK* E13;A20 Leu1196Met and Cys1156Tyr mutations. Each of these mutations leads to greater ALK fusion protein baseline phosphorylation suggesting that these mutations increase protein kinase activity. Both mutations reduce the sensitivity of these kinases to crizotinib and to a lesser extent to X-396. For cells expressing the EML4-ALK E13;A20 Leu1196Met mutant, the IC_{50} was 106 nM for X-396 *versus* 1820 nM for crizotinib. For cells expressing the EML4-ALK E13;A20 Cys1156Tyr mutant, the IC_{50} was 48 nM for X-396 *versus* 458 nM for crizotinib. Because the therapeutic window is greater for X-396, these results suggest that this drug may overcome these drug resistant mutations. X-396 is currently undergoing clinical trials for non-small cell lung cancer and for inflammatory myofibroblastic tumors (www.clinicaltrials.gov).

7.6. ASP3026

Kuromitsu et al. described ASP3026 as an orally effective heterocyclic 1,3,5-triazene-based (Fig. 7E, Astellas Pharma US, Inc.) ALK protein-tyrosine kinase targeted drug [140]. They indicated that the compound potently inhibits ALK kinase activity and is more selective than crizotinib in a protein kinase panel. In an anchorage independent *in vitro* cell growth assay, ASP3026 inhibits the growth of NCI-H2228 NSCLC tumor cells expressing EML4-ALK variant 3 and that of murine fibroblast NIH 3T3 cells expressing EML4-ALK variants 1, 2 and 3. These investigators found that ASP3026 (10 mg/kg for 14 days) induced marked tumor regression in mice bearing subcutaneous NCI-H2228 tumor xenografts with no effect on body weight. They also reported that the drug was effective against tumors bearing the Leu1196Met ALK gatekeeper mutation. The drug is currently in stage I clinical trials for B-cell lymphomas, immunoproliferative disorders, and non-Hodgkin lymphomas (www.clinicaltrials.gov).

7.7. GSK1838705

Sabbatini et al. reported that GSK1838705 is an orally effective pyrrolopyrimidine derivative (Fig. 7F, GlaxoSmithKlein) that inhibits ALK (IC_{50} = 0.5 nM), the insulin receptor (2 nM), and the insulin-like growth factor receptor (1.6 nM) protein-tyrosine kinase activities [141]. These investigators found that the drug inhibits several anaplastic large-cell lymphoma cell lines (L-82, SUP-M2, SU-DHL-1, Karpas-299, and SR-786) expressing the NPM-ALK fusion protein in a concentration-dependent fashion with IC_{50} values of 24–88 nM. They reported that H2228 NSCLC cells expressing the EML4-ALK are less sensitive to GSK1838705 (IC_{50} = 191 nM). The human CD30-positive T cell FE-PD line, which was established from an aggressive anaplastic large-cell lymphoma lacking an ALK

fusion protein, was relatively insensitive to the drug with an IC_{50} greater than 4 μM. These investigators found that GSK1838705 decreases tumor growth in mice bearing Karpas-299 or SR-786 xenografts in a dose-dependent fashion and without any weight loss. Sabbatini et al. found that drug treatment of mice has transient effects on blood glucose levels, most likely owing to its blockade of insulin signaling [141]. Chronic treatment of mice leads to hyperinsulinemia, which is required to maintain glucose homeostasis. These effects on insulin action decrease the likelihood that this compound will be therapeutically useful in the clinical setting.

7.8. CEP-28122 or compound **25b**

Cheng et al. reported that CEP-28122 (compound **25b**) is an orally effective diaminopyrimidine derivative (Fig. 7G, Cephalon, Inc.) that inhibits ALK protein kinase activity [142]. Gingrich et al. reported that the IC_{50} value is 1.9 nM for inhibition of enzyme activity *in vitro* and 20 nM for enzyme activity in cells [143]. This drug inhibits Flt4 protein-tyrosine kinase with an IC_{50} of 46 nM but it has little effect on a large number of other protein kinases [142]. However, CEP-28122 inhibits RSK2 (IC_{50} = 12 nM), RSK3 (7 nM), and RSK4 (17 nM) ribosomal s6 (protein-serine/threonine) kinases with low nanomolar IC_{50} values [142]. Cheng et al. reported that the compound induces apoptosis in anaplastic large-cell lymphoma Sup-M2 ($IC_{50} \approx 18$ nM) and in Karpas-299 (56 nM) cells, which are both NPM-ALK-positive, following treatment for 48–72 h [142]. However, the drug had little effect on two NPM-ALK negative cells lines (Toledo and Hut-102). Both studies demonstrated that orally administered CEP-28112 (30 mg/kg twice daily) inhibits the growth of a number of xenografts in athymic nude mice [142,143]. These include NPM-ALK-positive anaplastic large-cell lymphoma Sup-M2 cells and NSCLC EML4-ALK NCI-H228, NCI-H3122, and NCI-H1650 cells, and neuroblastoma NB-1 cells with ALK amplification, but not neuroblastoma NB-1691 cells with non-amplified wild type ALK [142]. CEP-28112 induces apoptosis in neuroblastoma SH-SY5Y cells bearing the crizotinib resistant Phe1174Leu mutation and NB-1643 cells bearing the crizotinib resistant Arg1275Gln mutation with IC_{50} values of 30 nM in each case [143]. A single oral dose (30 mg/kg) leads to more than 90% inhibition of NPM-ALK phosphorylation extending to 12 h in NPM-ALK-positive Karpas-299 tumor xenografts in nude mice. Moreover, administration of CEP-28112 (30 mg/kg twice daily) leads to complete tumor regression of Karpas-299 tumor xenografts in the absence of body weight changes or other overt signs of toxicity.

7.9. Cephalon compound **30**

Ott et al. reported that Cephalon **30** is an orally effective pyrrolotriazine derivative (Fig. 7H) that targets ALK kinase activity [144]. These investigators found that the IC_{50} value is 10 nM for inhibition of enzyme activity *in vitro* and 60 nM for enzyme activity in cells. The drug has little effect on the activity of the insulin receptor and a variety of other protein kinases. Compound **30** displayed concentration-dependent growth inhibition of human ALCL Sup-M2 (IC_{50} = 87 nM) and Karpas-299 (477 nM) cells in culture, but it had minimal inhibitory activity on ALK-negative human chronic myelogenous leukemia K562 cells. These data suggest that the drug exerts growth inhibition primarily through the inhibition of NPM-ALK activity. Compound **30** also promotes apoptosis in the two ALK-positive cell lines. Its oral bioavailability in both mouse and rat is about 35%. A single oral dose (30 mg/kg) produced a 75% decrease in NPM-ALK phosphorylation in Sup-M2 tumor xenografts in athymic nude mice. Oral administration leads to dose-dependent xenograft tumor regression in mice in the absence of weight loss or other signs of toxicity.

7.10. Amgen compounds **36** and **49**

Lewis et al. reported that these orally effective 2-acyliminobenzimidazoles (Fig. 7I and J) target ALK protein-tyrosine kinase activity [145]. They found that the IC_{50} value for inhibition of enzyme activity *in vitro* for **36** is 1.2 nM and for **49** is 1.0 nM. They reported that the IC_{50} value for inhibition of enzyme activity in cells for **36** is 4 nM and for **49** is 6 nM. Compounds **36** (IC_{50} = 536 nM) and **49** (231 nM) are much less potent against the insulin receptor kinase activity in cells. Both compounds demonstrated high selectivity for ALK in a kinome panel of 442 human protein kinases. For leukocyte tyrosine kinase, which most closely resembles ALK, compound **36** had a seven-fold and compound **49** had a 34-fold selectivity for ALK as determined by their respective K_d values. Compound **36** is rapidly cleared from mouse plasma owing to a murine-specific amidase that catalyzes the cleavage of its benzamidine group. Compound **49**, which is resistant to this cleavage, demonstrated dose-dependent Karpas-299 NPM-ALK tumor xenograft growth inhibition. At a dose of 30 mg/kg once daily, these investigators observed an 89% growth inhibition measured after 15 days of treatment. Moreover, the mice exhibited no overt signs of toxicity or weight loss after 15 days of once daily drug administration (60 mg/kg).

7.11. LDK378

LDK378 (Novartis) is an ALK inhibitor that is undergoing clinical trials in ALK activated non-small cell lung cancer and tumors characterized by genetic abnormalities of ALK (www.clinicaltrials.gov). However, because its structure and properties have not been reported in the public domain, it cannot be discussed further.

8. ALK inhibitor properties

8.1. Lipinski's rule of five

Pharmacologists and medicinal chemists have searched for drug-like chemical properties that result in compounds with therapeutic efficacy in a predictable fashion. Lipinski's rule represents an experimental and computational approach to estimate solubility, permeability, and efficacy in the drug discovery and development setting [146]. In the discovery setting the "rule of 5" predicts that poor absorption or permeation is more likely when there are more than 5 hydrogen-bond donors, 10 (5×2) hydrogen-bond acceptors, a molecular weight greater than 500 (5×100) and a calculated Log *P* (cLog *P*) greater than 5. The number of hydrogen-bond donors is expressed as the sum of OH and NH groups, and the number of hydrogen-bond acceptors is expressed as the sum of nitrogen (N) and oxygen (O) atoms. The "rule of 5" was empirically based on the properties of more than 2000 drugs [146]. Lipinski et al. noted that drugs that are substrates for biological transporters are exceptions to the rule.

Of the 11 ALK inhibitors considered in this review, only three of them (crizotinib, CH5424802, and Chugai compound **13d**) have molecular weights less than 500 (Table 9). Furthermore, three inhibitors have more than 10 hydrogen bond acceptors (ASP3026, GSK1838705, Cephalon compound **30**). It seems likely that suitable modification of the eight ALK inhibitors falling outside of the "rule of 5" criteria would result in better drugs.

8.2. The importance of lipophilicity

8.2.1. Lipophilic efficiency (LipE)

Since Lipinski's publication in 1997 [146], a deeper understanding of the physicochemical contributions to drug-likeness has led to the refinement of the rule of 5 [147]. The concept of

Table 9
Properties of ALK kinase inhibitors.

Drug or compound	Company	MW	D/A[a]	cLog P[b]	cLog D[b]	pK_i	LipE (K_i)	LE (K_i)	$-$Log IC_{50}	LipE (IC_{50})	LE (IC_{50})	Refs.[c]
Crizotinib	Pfizer	450	3/6	4.39	2.66	9.16	6.50	0.431	7.70	5.04	0.362	[113,135]
CH5424802	Chugai	483	1/6	5.48	5.24	8.72	3.48	0.333	8.52	3.28	0.326	[137]
13d	Chugai	469	1/6	4.93	4.88	8.54	3.66	0.345	7.89	3.01	0.319	[139]
AP26113	Ariad	529	2/8	4.08	3.00	10.0	7.00	0.393	8.02	5.02	0.315	[135]
X-396	Xcovery	547	3/9	4.08	3.61	9.40	5.79	0.359	8.04	4.43	0.307	[130]
ASP3026	Astellas	581	2/11	4.00	3.10	NR	NR	NR	NR	NR	NR	[140]
GSK1838705	GlaxoSmithKline	533	4/11	3.23	3.04	9.30	6.26	0.337	7.44	4.40	0.270	[141]
CEP-28122	Cephalon	539	4/9	5.03	4.57	8.72	4.15	3.24	7.69	3.12	2.86	[142,143]
30	Cephalon	568	2/11	3.28	3.06	8.00	4.94	0.283	7.22	4.16	0.255	[144]
36	Amgen	578	3/8	4.81	4.14	8.92	4.78	0.300	8.40	4.26	0.283	[145]
49	Amgen	596	3/8	5.16	4.51	9.00	4.49	0.296	8.22	3.73	0.270	[145]

[a] D, number of hydrogen bond donors; A, number of hydrogen-bond acceptors; MW, molecular weight; NR, not reported.
[b] Calculations performed with MedChem Designer™, version 2.0, Simulationsplus, Inc., Lancaster, CA 93534, USA.
[c] Sources of primary data on which the calculations are based.

lipophilic efficiency, or LipE, is a useful check on the tendency to use lipophilicity-driven binding to increase potency. The formulas for calculating lipophilic efficiency are given in Section 7.1.2. The first term is minus the log of the K_d, K_i, or IC_{50}; larger values indicate greater potency. Although these terms are often used interchangeably, they differ in definition and in value. When comparing a series of drugs during development, it is best to use the same assay to make valid comparisons. The K_d, or dissociation constant, is measured biochemically and represents an equilibrium constant. The K_i is also measured biochemically and is often reported as an "apparent" constant ($^{app}K_i$) because the value depends upon the concentrations of substrates during an assay. For example, if the drug is a competitive inhibitor with respect to one of the substrates, increasing the concentration of that substrate will decrease inhibition and increase the apparent K_i. The IC_{50} is the concentration of compound that inhibits a process by 50%. It can be determined biochemically for an enzyme *in vitro* or in a cell. Its value *in vitro* can change as a function of substrate concentrations. However, substrate concentrations in the cell, in general, cannot be controlled or readily varied.

The second term ($-$cLog D or minus cLog D) represents the lipophilicity of a compound or drug where c indicates that the value is calculated, or computed, using an algorithm based upon the behavior of thousands of organic compounds, and D is the distribution coefficient determined at a particular pH. This term is the log of the ratio of the solubility of the compound in octanol/water. The more soluble the compound is in octanol, the greater is its lipophilicity, and the greater is the value of $-$cLog D. Leeson and Springthorpe suggest that compound lipophilicity, as estimated by $-$cLog P, is the most important chemical property to consider during drug development [148]. Their use of $-$cLog P was based upon results obtained prior to the use of D, the distribution coefficient. Lipophilicity plays a dominant role in promoting binding to unwanted drug targets. The goal for drug optimization in the developmental stage is to increase potency without simultaneously increasing lipophilicity.

cLog D can be determined for several compounds *in silico* in a matter of minutes; the experimental determination of Log D is time-consuming and is performed only in select cases. Optimal values of LipE range from 5 to 10 [147]. Increasing potency and decreasing the lipophilicity during drug development, in general, lead to better pharmacological properties. The values of LipE calculated on the basis of biochemical (K_i) and cellular (IC_{50}) assays for 11 ALK inhibitors are given in Table 9. Although several of the drugs have biochemical LipE values greater than 5, only crizotinib and AP26113 have cellular LipE (IC_{50}) values greater than 5.

8.2.2. Ligand efficiency (LE)

The ligand efficiency (LE), which is a key molecular property, is a measurement that relates the potency per heavy atom (non-hydrogen atom) in a drug. The ligand efficiency is given by the following equation:

$$\mathrm{LE} = \frac{\Delta G^{\circ\prime}}{N} = -RT\ \ln\frac{K_{eq}}{N} = -2.303RT\,\mathrm{Log}_{10}\frac{K_{eq}}{N} \quad (3)$$

$\Delta G^{\circ\prime}$ represents the standard free energy change at pH 7 during the binding of a drug to its target, N is the number of non-hydrogen atoms ("heavy atoms") in the drug, R is the universal temperature-energy coefficient, or gas constant (1.98 cal/° mol, or 0.00198 kcal/° mol), T is the absolute temperature in Kelvin, and K_{eq} is the equilibrium constant. Ideal values of LE are greater than 0.3 (in kcal/mol). Since it is rarely possible or practical to measure the equilibrium constant, the K_i or IC_{50} are used instead. At 37 °C, or 310 K, Eq. (3) becomes $-(2.303 \times (0.00198\ \mathrm{kcal/mol\,K}) \times 310\ \mathrm{K}\,\mathrm{Log}_{10}K_{eq})/N$ or $-1.41\,\mathrm{Log}_{10}K_{eq}/N$.

The ligand efficiency represents the relative binding affinity per non-hydrogen atom in the drug or compound of interest. The value of N serves as a surrogate for the molecular weight. The lower the value of N, the smaller the molecular weight, and the larger is the ligand efficiency. The greater the potency or binding affinity, the greater is $-\mathrm{Log}_{10}K_{eq}$, and the larger is the ligand efficiency. The values of LE calculated on the basis of biochemical (K_i) and cellular (IC_{50}) assays for the drugs listed in Section 7 are given in Table 9. The first five drugs listed have favorable cell-based (IC_{50}) ligand efficiencies (>0.3), while several others have biochemical values (K_i) in excess of 0.3. It appears that the cell-based value is a more stringent criterion in the assessment of candidate compounds.

The values for lipophilic efficiency (LipE) and ligand efficiency (LE) listed in Table 9 are calculated from experiments performed under a variety of different conditions. Therefore LipE and LE values alone cannot be used to make a direct comparison of the drugs because of these differences in methodology. The examples were derived from various drug discovery efforts and are meant to provide representative values. Cui et al. used LipE and LE as two of their parameters during the development of crizotinib as a c-Met inhibitor [113]. They used the same biochemical assays and same cells under identical conditions for the calculation of LipE and LE for dozens of compounds on their pathway to crizotinib, thus making choices for lead optimization more efficient.

9. Development of small molecule protein kinase inhibitors

9.1. The comparative effectiveness of protein kinase inhibitors against targeted diseases and the development of acquired drug resistance

The Philadelphia chromosome occurs in about 95% of chronic myelogenous leukemia cases. Rowley discovered that the Philadelphia chromosome was produced by a reciprocal translocation t(9;22)(q34;q11.2) that results in a shortened chromosome 22 (the Philadelphia chromosome) and a lengthened chromosome 9 [149]. This translocation leads to the formation of the BCR-Abl oncogene where BCR refers to breakpoint cluster region, which was originally on chromosome 22, and Abl is the human ortholog of the murine Abelson leukemia virus, which was originally on chromosome 9 [150,136]. As a result of the formation of the fusion protein, the BCR-Abl kinase exhibits increased activity and is the dominant factor in the pathogenesis of the disease.

The natural history of chronic myelogenous leukemia is one of slow progression and a median survival of three years without treatment. The disease consists of three phases: chronic, accelerated, and blast crisis [151]. After a variable chronic phase of a few years, about 50% of people enter an accelerated phase of 6–12 months duration terminating in a blast crisis. The other 50% of patients enter the blast crisis directly, and in both situations the crisis behaves like an acute leukemia and rapidly progresses to death. Disease progression is most likely due to mutations that occur after the BCR-Abl translocation.

Imatinib is an ATP-competitive inhibitor of BCR-Abl and is effective in the treatment of the chronic phase of the disorder [136]. Hughes et al. reported that the overall seven-year survival rate was 86% in those people who received the drug [152]. However, Khorashad and Deininger estimated that 20–40% of newly diagnosed chronic phase individuals develop intolerance (toxic side effects occur in ≈2% of cases) or resistance to imatinib [151]. On the favorable side, this indicates that 60–80% of people with chronic myelogenous leukemia will receive a long-term clinical benefit that will potentially last for a decade or more.

Although imatinib was the first approved small molecule protein kinase inhibitor, it has better therapeutic properties than most subsequently approved protein kinase inhibitors in terms of (a) its effectiveness (greater than 95% complete hematological response [153]) against its target disease (chronic myelogenous leukemia) and (b) the relative lack of development of drug resistance when compared with inhibitors targeting kinases other than BCR-Abl. Several mechanisms of resistance to imatinib have been described [154]. These can be classified as BCR-Abl-dependent or BCR-Abl-independent. The first group includes amplification or overexpression of BCR-Abl or point mutations in the Abl protein kinase sequence. The second group includes decreased cellular uptake, increased drug efflux, or upregulation of alternative signaling pathways such as the Ras/Raf/MEK/ERK1/2 and Src family kinase pathways [155]. Point mutations are the most common mechanism for the development of imatinib resistance. More than 100 different mutations have been described, and they occur in several domains of the kinase including the ATP-binding site, the catalytic segment, the activation segment, and amino acids that make direct contact with imatinib.

Owing to the development of BCR-Abl mutants to which imatinib is unable to inhibit, second generation inhibitors including dasatinib and nilotinib have been developed and approved for the treatment of BCR-Abl-positive chronic myelogenous leukemia [155]. Ohanian et al. suggested that either of these drugs be given as first line therapy because they are more potent and have higher optimal response rates when compared with imatinib [155]. Furthermore, dasatinib is effective against the Tyr253His and Glu255Lys/Val glycine-rich loop mutants and the Phe359Cys/Ile/Val catalytic domain imatinib-resistant mutants; nilotinib is effective against the Val299Leu β4–β5 loop mutant, the Thr315Ala gatekeeper mutant, and the Phe317Cys/Ile/Leu/Val hinge region imatinib-resistant mutants. Bosutinib is a BCR-Abl inhibitor that was approved in 2012 for the treatment of Philadelphia chromosome positive chronic myelogenous leukemia (www.accessdata.fda.gov/drugsatfda_docs/label/2012/203341lbl.pdf). Bosutinib seems to be effective against the Phe317 and the Phe369 BCR-Abl mutants. Unfortunately, none of these three second-generation approved drugs is effective against the BCR-Abl Thr315Ile gatekeeper mutation. Mutations of the six residues listed in this paragraph account for about two-thirds of the more than 100 described BCR-Abl mutations. Imatinib, with an annual cost of $32,000–$98,000 in the US, will come off of its patent in 2015 and its expected lower cost may be a factor in its therapeutic use.

The overall response rate for crizotinib in the treatment of ALK-positive NSCLC patients was 57% ($N = 82$), which is much lower than the response rate for imatinib of greater than 95%. Katayama et al. reported that crizotinib resistance occurred in all ALK-positive NSCLC patients ($N = 18$) studied with a range of 4–34 months and a median of 10.5 months [125]. Only 28% of crizotinib resistance was due to mutations in the protein kinase domain or to *EML4-ALK* gene amplification. The other possible modes of resistance are related to upregulation of alternative signaling pathways or to unknown mechanisms. In the case of ALK and other protein kinase inhibitor targets, it may be possible to develop other drugs that inhibit mutant kinases, but other strategies will have to be employed to block the other modes of drug resistance.

Dysregulation of EGFR kinase activity has been implicated in the oncogenic transformation of cells [156]. Moreover, amplification or activation of EGFR has been observed in non-small cell lung cancer (NSCLC). Erlotinib and gefitinib have been approved by the US Food and Drug Administration for the treatment of people with NSCLC. Nevertheless, people initially responding to therapy invariably develop resistance to these drugs, thereby limiting progression-free survival to 9–13 months with a median survival duration of 2 years [157]. Pao et al. reported that the chief molecular mechanism responsible for drug resistance includes the acquisition of a secondary Thr790Met mutation in the EGFR kinase domain [158]. However, this constitutes about half of the EGFR drug-resistant cases, which indicates that other mechanisms exist that lead to drug resistance such as stimulation of c-Met signaling.

Unlike BCR-Abl and ALK, EGFR mutations conferring drug resistance involve only the gatekeeper residue, while mutations conferring drug resistance in BCR-Abl and ALK are many and varied. Unlike the case for imatinib and BCR-Abl, the EGFR Thr790Met gatekeeper mutation does not block access to a hydrophobic pocket next to the ATP-binding site. A Leu858Arg or a Gly719Ser mutation or a small in-frame deletion of exon 19 leads to the expression of activated EGFRs that are sensitive to gefitinib and erlotinib [159]. These mutant proteins exhibit a decrease in affinity for ATP during catalysis (an increase in the concentration of ATP at half maximal velocity, or K_m) and are thus less able to block the binding of the ATP competitive inhibitors at physiological ATP concentrations. Yun et al. reported that the affinity of gefitinib was greater for the gatekeeper mutant ($K_i = 4.6$ nM), the activated Leu858Arg mutant ($K_i = 2.4$ nM), and the drug-resistant Leu858Arg/Thr790Met double mutant ($K_i = 10.9$ nM) than for the wild type enzyme ($K_i = 35.3$ nM) [159]. The Leu858Arg mutant has an elevated K_m for ATP of 148 μM when compared with the wild type ($K_m = 5.2$ μM), the Thr790Met gatekeeper mutant ($K_m = 5.9$ μM), and the Leu858Arg/Thr790Met drug-resistant double mutant ($K_m = 8.4$ μM). The secondary gatekeeper mutation in the primary Leu858Arg activating mutation thus restores gefitinib sensitivity by increasing the ability of ATP

to more effectively compete with drug binding during catalysis. As is the case for ALK described in Section 7.1.4, mutation of the EGFR gatekeeper to methionine activates protein kinase activity.

Vemurafenib is used in the treatment of melanoma that results from the B-Raf (Val600Glu) mutation with an overall response rate of about 69% ($N = 16$) [160]. Tuma reported that nearly all people develop resistance to the drug between 2 and 18 months with a median duration of response of 6.2 months [161]. Surprisingly, resistance occurs in the absence of secondary mutations in the B-Raf kinase domain [3], and the lack of kinase domain drug-resistant mutations is a unique property of B-Raf (Val600Glu) among protein kinase targets. The mechanisms of B-Raf inhibitor resistance include the development of activated *N-Ras* mutants, overexpression of the COT protein serine/threonine kinase, upregulation of PDGFRβ or the insulin-like growth factor receptor, upregulation of the B-Raf Val600Glu mutant (the primary drug target), or the development of an alternatively spliced B-Raf Val600Glu enzyme that fails to bind or be inhibited by vemurafenib [3]. Thus, each type of neoplasm has its own unique biology and its own pathways leading to drug resistance.

9.2. The role of serendipity in successful protein kinase inhibitor development

Imatinib was initially developed as a PDGFR inhibitor, but its initially approved therapeutic targets include BCR-Abl [136] and Kit [46]. Imatinib was approved in 2000 for the treatment of BCR-Abl-positive chronic myelogenous leukemia and in 2005 for the treatment of gastrointestinal stromal tumors with Kit gain-of-function mutations in the juxtamembrane segment [46,136]. The drug has subsequently been approved by the US Food and Drug Administration for the treatment of a variety of other diseases including adults with (a) refractory Philadelphia chromosome positive acute lymphoblastic leukemia, (b) myeloproliferative diseases associated with *PDGFR* gene rearrangements, (c) aggressive systemic mastocytosis, (d) chronic eosinophilic leukemia, and (e) dermatofibrosarcoma protuberans (www.accessdata.fda.gov/scripts/cder/drugsatfda/).

Sorafenib was initially developed as a Raf inhibitor, but it inhibits several protein kinases including Flt3, Kit, PDGFRβ, and VEGFR1/2/3 [3]. This drug is approved for the treatment of renal cell carcinoma and for hepatocellular carcinoma [3]. Its effectiveness against renal cell carcinoma is through its inhibition of the VEGF receptors (inhibition of angiogenesis), and its effectiveness against hepatocellular carcinoma may involve the inhibition of VEGFR2/3, PDGFRβ, and B/C-Raf in the Ras/Raf/MEK/ERK1/2 signal transduction pathway.

As noted in Section 7.1.2, crizotinib was developed by structure-based drug design to inhibit c-Met [113]. It is now approved for the treatment of EML4-ALK-positive NSCLC. Crizotinib is undergoing or has undergone more than three dozen clinical trials (www.clinicaltrials.gov). Targeted diseases include locally advanced and/or metastatic (a) anaplastic large-cell lymphoma, (b) inflammatory myofibroblastic tumor, (c) papillary renal cell carcinoma, (d) alveolar rhabdomyosarcoma, and (e) neuroblastoma, (f) brain and central nervous system tumors, (g) and lung cancer. The studies outlined in Section 7.1 failed to demonstrate an anti-tumor effect based upon c-Met inhibition. However, c-Met represents an attractive drug target, and future studies may reveal a therapeutic effect based upon c-Met inhibition.

Although it is counterintuitive, the success of these drugs is related in part to their lack of selectivity and their ability to inhibit more than one protein kinase. It is also possible that their therapeutic effectiveness is related to the simultaneous inhibition of more than a single enzyme.

9.3. Rapid timeline in the development of crizotinib therapy for EML4-ALK-positive non-small cell lung cancer

Soda et al. first reported the discovery of an EML4-ALK fusion protein in non-small cell lung cancers in 2007 [11]. At the same time, Christensen et al. and Zou et al. were examining the effects of crizotinib in cells and in animals on tumor growth mediated by activated c-Met and ALK [121,162]. Within three years, Kwak et al. and Choi et al. reported that EML4-ALK-positive NSCLC patients exhibited a response rate of about 55% from oral crizotinib [122,127].

Gerber and Mina compared the development of crizotinib with that of imatinib, erlotinib, and vemurafenib and contrasted the interval between drug target discovery and the documentation of drug target inhibition [163]. The BCR-Abl protein kinase was discovered in 1984, and its first clinically effective inhibitor (imatinib) was shown to block this activity 16 years later (2000) [164]. That EGFR participates in malignant transformation was known by 1995, and its inhibition by erlotinib and gefitinib was established within nine years (2004) [96]. The role of B-Raf mutations in melanoma was discovered in 2002, and clinically effective inhibitors were identified eight years later (2010) [165]. That Kit participates in the pathogenesis of gastrointestinal stromal tumors was discovered in 1998, and a clinically effective candidate was identified within four years (2002); the first approved Kit inhibitor was imatinib, a drug that was previously approved for the treatment of chronic myelogenous leukemia [46].

The EML4-ALK fusion protein was discovered in NSCLCs in 2007 [11], and a clinically effective inhibitor (crizotinib) was identified in 2010 [122,127]. The US Food and Drug Administration approved crizotinib for first-line therapy in August 2011. It is unlikely that much can be done to increase this rate of translation from the laboratory to the clinic because of the time required for clinical trails to demonstrate therapeutic efficacy, but the experience gained from various protein kinase drug discovery programs undoubtedly aids in this process.

10. Epilogue

There are more than 500 protein kinases in the human genome [1]. Several dozen kinases are implicated in the pathogenesis of cancer, diabetes, and autoimmune, cardiovascular, inflammatory, and nervous disorders. There are currently 250 or more protein kinase inhibitors in various stages of clinical development worldwide. Nearly all of the US Food and Drug Administration currently approved drugs are used for the treatment of neoplastic disorders with the exception of tofacitinib, which is used in the treatment of rheumatoid arthritis. We can expect advances in clinical efficacy and subsequent approval of new drugs targeting a wider array of protein kinases and diseases in both the near and distant future.

Conflict of interest

The author is unaware of any affiliations, memberships, or financial holdings that might be perceived as affecting the objectivity of this review.

Acknowledgments

The author thanks Dr. J. Jean Cui for insightful discussion and Laura M. Roskoski for bibliographic and editorial assistance.

References

[1] Manning G, Whyte DB, Martinez R, Hunter T, Sudarsanam S. The protein kinase complement of the human genome. Science 2002;298:1912–34.

[2] Alonso A, Sasin J, Bottini N, Friedberg I, Friedberg I, Osterman A, et al. Protein tyrosine phosphatases in the human genome. Cell 2004;117:699–711.
[3] Roskoski Jr R. ERK1/2 MAP kinases: structure, function, and regulation. Pharmacological Research 2012;66:105–43.
[4] Taylor SS, Keshwani MM, Steichen JM, Kornev AP. Evolution of the eukaryotic protein kinases as dynamic molecular switches. Philosophical Transactions of the Royal Society London Biological Science 2012;367:2517–28.
[5] Aleshin AE, Malfois M, Liu X, Kim CS, Fromm HJ, Honzatko RB, et al. Nonaggregating mutant of recombinant human hexokinase I exhibits wild-type kinetics and rod-like conformations in solution. Biochemistry 1999;38: 8359–66.
[6] Fujioka A, Terai K, Itoh RE, Aoki K, Nakamura T, Kuroda S, et al. Dynamics of the Ras/ERK MAPK cascade as monitored by fluorescent probes. Journal of Biological Chemistry 2006;281:8917–26.
[7] Grant BD, Adams JA. Pre-steady-state kinetic analysis of cAMP-dependent protein kinase using rapid quench flow techniques. Biochemistry 1996;35:2022–9.
[8] Lemmon MA, Schlessinger J. Cell signaling by receptor tyrosine kinases. Cell 2010;141:1117–34.
[9] Morris SW, Kirstein MN, Valentine MB, Dittmer K, Shapiro DN, Look AT, et al. Fusion of a kinase gene, ALK, to a nucleolar protein gene, NPM, in non-Hodgkin's lymphoma. Science 1995;267:316–7.
[10] Shiota M, Fujimoto J, Semba T, Satoh H, Yamamoto T, Mori S. Hyperphosphorylation of a novel 80 kDa protein-tyrosine kinase similar to Ltk in a human Ki-1 lymphoma cell line, AMS3. Oncogene 1994;9:1567–74.
[11] Soda M, Choi YL, Enomoto M, Takada S, Yamashita Y, Ishikawa S, et al. Identification of the transforming EML4-ALK fusion gene in non-small-cell lung cancer. Nature 2007;448:561–6.
[12] Rikova K, Guo A, Zeng Q, Possemato A, Yu J, Haack H, et al. Global survey of phosphotyrosine signaling identifies oncogenic kinases in lung cancer. Cell 2007;131:1190–203.
[13] Tabbó F, Barreca A, Piva R, Inghirami G, European T-Cell Lymphoma Study Group. ALK signaling and target therapy in anaplastic large cell lymphoma. Frontiers in Oncology 2012;2:41.
[14] Chen Y, Takita J, Choi YL, Kato M, Ohira M, Sanada M, et al. Oncogenic mutations of ALK kinase in neuroblastoma. Nature 2008;455:971–4.
[15] George RE, Sanda T, Hanna M, Fröhling S, Luther 2nd W, Zhang J, et al. Activating mutations in ALK provide a therapeutic target in neuroblastoma. Nature 2008;455:975–8.
[16] Janoueix-Lerosey I, Lequin D, Brugières L, Ribeiro A, de Pontual L, Combaret V, et al. Somatic and germline activating mutations of the ALK kinase receptor in neuroblastoma. Nature 2008;455:967–70.
[17] Mossé YP, Laudenslager M, Longo L, Cole KA, Wood A, Attiyeh EF, et al. Identification of ALK as a major familial neuroblastoma predisposition gene. Nature 2008;455:930–5.
[18] Morris SW, Naeve C, Mathew P, James PL, Kirstein MN, Cui X, et al. ALK, the chromosome 2 gene locus altered by the t(2;5) in non-Hodgkin's lymphoma, encodes a novel neural receptor tyrosine kinase that is highly related to leukocyte tyrosine kinase (LTK). Oncogene 1997;14:2175–88. Erratum in: Oncogene 1997;15:2883.
[19] Mano H. ALKoma: a cancer subtype with a shared target. Cancer Discovery 2012;2:495–502.
[20] Lorén CE, Englund C, Grabbe C, Hallberg B, Hunter T, Palmer RH. A crucial role for the anaplastic lymphoma kinase receptor tyrosine kinase in gut development in *Drosophila melanogaster*. EMBO Reports 2003;4:781–6.
[21] Stoica GE, Kuo A, Aigner A, Sunitha I, Souttou B, Malerczyk C, et al. Identification of anaplastic lymphoma kinase as a receptor for the growth factor pleiotrophin. Journal of Biological Chemistry 2001;276:16772–9.
[22] Stoica GE, Kuo A, Powers C, Bowden ET, Sale EB, Riegel AT, et al. Midkine binds to anaplastic lymphoma kinase (ALK) and acts as a growth factor for different cell types. Journal of Biological Chemistry 2002;277:35990–8.
[23] Motegi A, Fujimoto J, Kotani M, Sakuraba H, Yamamoto T. ALK receptor tyrosine kinase promotes cell growth and neurite outgrowth. Journal of Cell Science 2004;117:3319–29.
[24] Moog-Lutz C, Degoutin J, Gouzi JY, Frobert Y, Brunet-de Carvalho N, Bureau J, et al. Activation and inhibition of anaplastic lymphoma kinase receptor tyrosine kinase by monoclonal antibodies and absence of agonist activity of pleiotrophin. Journal of Biological Chemistry 2005;280:26039–48.
[25] Iwahara T, Fujimoto J, Wen D, Cupples R, Bucay N, Arakawa T, et al. Molecular characterization of ALK, a receptor tyrosine kinase expressed specifically in the nervous system. Oncogene 1997;14:439–49.
[26] Vernersson E, Khoo NK, Henriksson ML, Roos G, Palmer RH, Hallberg B. Characterization of the expression of the ALK receptor tyrosine kinase in mice. Gene Expression Patterns 2006;6:448–61.
[27] Bilsland JG, Wheeldon A, Mead A, Znamenskiy P, Almond S, Waters KA, et al. Behavioral and neurochemical alterations in mice deficient in anaplastic lymphoma kinase suggest therapeutic potential for psychiatric indications. Neuropsychopharmacology 2008;33:685–700.
[28] Lasek AW, Lim J, Kliethermes CL, Berger KH, Joslyn G, Brush G, et al. An evolutionary conserved role for anaplastic lymphoma kinase in behavioral responses to ethanol. PLoS One 2011;6(7):e22636.
[29] Knighton DR, Zheng JH, Ten Eyck LF, Ashford VA, Xuong NH, Taylor SS, et al. Crystal structure of the catalytic subunit of cyclic adenosine monophosphate-dependent protein kinase. Science 1991;253:407–14.
[30] Taylor SS, Kornev AP. Protein kinases: evolution of dynamic regulatory proteins. Trends in Biochemical Sciences 2011;36:65–77.
[31] Lee CC, Jia Y, Li N, Sun X, Ng K, Ambing E, et al. Crystal structure of the ALK (anaplastic lymphoma kinase) catalytic domain. Biochemical Journal 2010;430:425–37.
[32] Bossi RT, Saccardo MB, Ardini E, Menichincheri M, Rusconi L, Magnaghi P, et al. Crystal structures of anaplastic lymphoma kinase in complex with ATP competitive inhibitors. Biochemistry 2010;49:6813–25.
[33] Hanks SK, Quinn AM, Hunter T. The protein kinase family: conserved features and deduced phylogeny of the catalytic domains. Science 1988;241:42–52.
[34] Kornev AP, Haste NM, Taylor SS, Eyck LF. Surface comparison of active and inactive protein kinases identifies a conserved activation mechanism. Proceedings of the National Academy of Sciences of the United States of America 2006;103:17783–8.
[35] Zhou J, Adams JA. Participation of ADP dissociation in the rate-determining step in cAMP-dependent protein kinase. Biochemistry 1997;36:15733–8.
[36] Schwartz PA, Murray BW. Protein kinase biochemistry and drug discovery. Bioorganic Chemistry 2011;39:192–210.
[37] Kornev AP, Taylor SS. Defining the conserved internal architecture of a protein kinase. Biochimica et Biophysica Acta 2010;1804:440–4.
[38] Zhang J, Yang PL, Gray NS. Targeting cancer with small molecule kinase inhibitors. Nature Reviews Cancer 2009;9:28–39.
[39] Hubbard SR, Wei L, Ellis L, Hendrickson WA. Crystal structure of the tyrosine kinase domain of the human insulin receptor. Nature 1994;372:746–54.
[40] Hubbard SR. Crystal structure of the activated insulin receptor tyrosine kinase in complex with peptide substrate and ATP analog. EMBO Journal 1997;16:5572–81.
[41] Huse M, Kuriyan J. The conformational plasticity of protein kinases. Cell 2002;109:275–82.
[42] Bresler SC, Wood AC, Haglund EA, Courtright J, Belcastro LT, Plegaria JS, et al. Differential inhibitor sensitivity of anaplastic lymphoma kinase variants found in neuroblastoma. Science Translational Medicine 2011;3(108):108ra114.
[43] Palmer RH, Vernersson E, Grabbe C, Hallberg B. Anaplastic lymphoma kinase: signalling in development and disease. Biochemical Journal 2009;420:345–61.
[44] Wei L, Hubbard SR, Hendrickson WA, Ellis L. Expression, characterization, and crystallization of the catalytic core of the human insulin receptor protein-tyrosine kinase domain. Journal of Biological Chemistry 1995;270:8122–30.
[45] Tartari CJ, Gunby RH, Coluccia AM, Sottocornola R, Cimbro B, Scapozza L, et al. Characterization of some molecular mechanisms governing autoactivation of the catalytic domain of the anaplastic lymphoma kinase. Journal of Biological Chemistry 2008;283:3743–50.
[46] Roskoski Jr R. Structure and regulation of Kit protein-tyrosine kinase – the stem cell factor receptor. Biochemical Biophysical Research Communications 2005;338:1307–15.
[47] Chiarle R, Voena C, Ambrogio C, Piva R, Inghirami G. The anaplastic lymphoma kinase in the pathogenesis of cancer. Nature Reviews Cancer 2008;8:11–23.
[48] Vanhaesebroeck B, Stephens L, Hawkins P. PI3K signalling: the path to discovery and understanding. Nature Reviews Molecular Cell Biology 2012;13:195–203.
[49] Singh RR, Cho-Vega JH, Davuluri Y, Ma S, Kasbidi F, Milito C, et al. Sonic hedgehog signaling pathway is activated in ALK-positive anaplastic large cell lymphoma. Cancer Research 2009;69:2550–8.
[50] Marzec M, Kasprzycka M, Liu X, Raghunath PN, Wlodarski P, Wasik MA. Oncogenic tyrosine kinase NPM/ALK induces activation of the MEK/ERK signaling pathway independently of c-Raf. Oncogene 2007;26:813–21.
[51] Fujimoto J, Shiota M, Iwahara T, Seki N, Satoh H, Mori S, et al. Characterization of the transforming activity of p80, a hyperphosphorylated protein in a Ki-1 lymphoma cell line with chromosomal translocation t(2;5). Proceedings of the National Academy of Sciences of the United States of America 1996;93:4181–6.
[52] Zhang Q, Raghunath PN, Xue L, Majewski M, Carpentieri DF, Odum N, et al. Multilevel dysregulation of STAT3 activation in anaplastic lymphoma kinase-positive T/null-cell lymphoma. Journal of Immunology 2002;168:466–74.
[53] Galkin AV, Melnick JS, Kim S, Hood TL, Li N, Li L, et al. Identification of NVP-TAE684, a potent, selective, and efficacious inhibitor of NPM-ALK. Proceedings of the National Academy of Sciences of the United States of America 2007;104:270–5. Erratum in: Proceedings of the National Academy of Sciences USA 2007;104:2025.
[54] Stein H, Mason DY, Gerdes J, O'Connor N, Wainscoat J, Pallesen G, et al. The expression of the Hodgkin's disease associated antigen Ki-1 in reactive and neoplastic lymphoid tissue: evidence that Reed-Sternberg cells and histiocytic malignancies are derived from activated lymphoid cells. Blood 1985;66:848–58.
[55] Ferreri AJ, Govi S, Pileri SA, Savage KJ. Anaplastic large cell lymphoma, ALK-positive. Critical Reviews in Oncology/Hematology 2012;83: 293–302.
[56] Cools J, Wlodarska I, Somers R, Mentens N, Pedeutour F, Maes B, et al. Identification of novel fusion partners of ALK, the anaplastic lymphoma kinase, in anaplastic large-cell lymphoma and inflammatory myofibroblastic tumor. Genes, Chromosomes and Cancer 2002;34:354–62.
[57] Hernández L, Pinyol M, Hernández S, Beà S, Pulford K, Rosenwald A, et al. TRK-fused gene (TFG) is a new partner of ALK in anaplastic large cell lymphoma producing two structurally different TFG-ALK translocations. Blood 1999;94:3265–8.
[58] Hernández L, Beà S, Bellosillo B, Pinyol M, Falini B, Carbone A, et al. Diversity of genomic breakpoints in TFG-ALK translocations in anaplastic large

cell lymphomas: identification of a new TFG-ALK(XL) chimeric gene with transforming activity. American Journal of Pathology 2002;160:1487–94.
[59] Tort F, Pinyol M, Pulford K, Roncador G, Hernandez L, Nayach I, et al. Molecular characterization of a new ALK translocation involving moesin (MSN-ALK) in anaplastic large cell lymphoma. Laboratory Investigation 2001;81:419–26.
[60] Tort F, Campo E, Pohlman B, Hsi E. Heterogeneity of genomic breakpoints in MSN-ALK translocations in anaplastic large cell lymphoma. Human Pathology 2004;35:1038–41.
[61] Lamant L, Dastugue N, Pulford K, Delsol G, Mariamé B. A new fusion gene TPM3-ALK in anaplastic large cell lymphoma created by a (1;2)(q25;p23) translocation. Blood 1999;93:3088–95.
[62] Siebert R, Gesk S, Harder L, Steinemann D, Grote W, Schlegelberger B, et al. Complex variant translocation t(1;2) with TPM3-ALK fusion due to cryptic ALK gene rearrangement in anaplastic large-cell lymphoma. Blood 1999;94:3614–7.
[63] Meech SJ, McGavran L, Odom LF, Liang X, Meltesen L, Gump J, et al. Unusual childhood extramedullary hematologic malignancy with natural killer cell properties that contains tropomyosin 4 – anaplastic lymphoma kinase gene fusion. Blood 2001;98:1209–16.
[64] Ma Z, Cools J, Marynen P, Cui X, Siebert R, Gesk S, et al. Inv(2)(p23q35) in anaplastic large-cell lymphoma induces constitutive anaplastic lymphoma kinase (ALK) tyrosine kinase activation by fusion to ATIC, an enzyme involved in purine nucleotide biosynthesis. Blood 2000;95:2144–9.
[65] Trinei M, Lanfrancone L, Campo E, Pulford K, Mason DY, Pelicci PG, et al. A new variant anaplastic lymphoma kinase (ALK)-fusion protein (ATIC-ALK) in a case of ALK-positive anaplastic large cell lymphoma. Cancer Research 2000;60:793–8.
[66] Colleoni GW, Bridge JA, Garicochea B, Liu J, Filippa DA, Ladanyi M. ATIC-ALK: a novel variant ALK gene fusion in anaplastic large cell lymphoma resulting from the recurrent cryptic chromosomal inversion, inv(2)(p23q35). American Journal of Pathology 2000;156:781–9.
[67] Lamant L, Gascoyne RD, Duplantier MM, Armstrong F, Raghab A, Chhanabhai M, et al. Non-muscle myosin heavy chain (MYH9): a new partner fused to ALK in anaplastic large cell lymphoma. Genes, Chromosomes and Cancer 2003;37:427–32.
[68] Touriol C, Greenland C, Lamant L, Pulford K, Bernard F, Rousset T, et al. Further demonstration of the diversity of chromosomal changes involving 2p23 in ALK-positive lymphoma: 2 cases expressing ALK kinase fused to CLTCL (clathrin chain polypeptide-like). Blood 2000;95:3204–7.
[69] Takeuchi K, Choi YL, Togashi Y, Soda M, Hatano S, Inamura K, et al. KIF5B-ALK, a novel fusion oncokinase identified by an immunohistochemistry-based diagnostic system for ALK-positive lung cancer. Clinical Cancer Research 2009;15:3143–9.
[70] Wong DW, Leung EL, Wong SK, Tin VP, Sihoe AD, Cheng LC, et al. A novel KIF5B-ALK variant in nonsmall cell lung cancer. Cancer 2011;117: 2709–18.
[71] Togashi Y, Soda M, Sakata S, Sugawara E, Hatano S, Asaka R, et al. KLC1-ALK: a novel fusion in lung cancer identified using a formalin-fixed paraffin-embedded tissue only. PLoS One 2012;7(2):e31323.
[72] Jung Y, Kim P, Jung Y, Keum J, Kim SN, Choi YS, et al. Discovery of ALK-PTPN3 gene fusion from human non-small cell lung carcinoma cell line using next generation RNA sequencing. Genes, Chromosomes and Cancer 2012;51:590–7.
[73] Lawrence B, Perez-Atayde A, Hibbard MK, Rubin BP, Dal Cin P, Pinkus JL, et al. TPM3-ALK and TPM4-ALK oncogenes in inflammatory myofibroblastic tumors. American Journal of Pathology 2000;157:377–84.
[74] Bridge JA, Kanamori M, Ma Z, Pickering D, Hill DA, Lydiatt W, et al. Fusion of the ALK gene to the clathrin heavy chain gene, CLTC, in inflammatory myofibroblastic tumor. American Journal of Pathology 2001;159: 411–5.
[75] Patel AS, Murphy KM, Hawkins AL, Cohen JS, Long PP, Perlman EJ, et al. RANBP2 and CLTC are involved in ALK rearrangements in inflammatory myofibroblastic tumors. Cancer Genetics and Cytogenetics 2007;176: 107–14.
[76] Debiec-Rychter M, Marynen P, Hagemeijer A, Pauwels P. ALK-ATIC fusion in urinary bladder inflammatory myofibroblastic tumor. Genes, Chromosomes and Cancer 2003;38:187–90.
[77] Debelenko LV, Arthur DC, Pack SD, Helman LJ, Schrump DS, Tsokos M. Identification of CARS-ALK fusion in primary and metastatic lesions of an inflammatory myofibroblastic tumor. Laboratory Investigation 2003;83: 1255–65.
[78] Ma Z, Hill DA, Collins MH, Morris SW, Sumegi J, Zhou M, et al. Fusion of ALK to the Ran-binding protein 2 (RANBP2) gene in inflammatory myofibroblastic tumor. Genes, Chromosomes and Cancer 2003;37:98–105.
[79] Mariño-Enríquez A, Wang WL, Roy A, Lopez-Terrada D, Lazar AJ, Fletcher CD, et al. Epithelioid inflammatory myofibroblastic sarcoma: an aggressive intra-abdominal variant of inflammatory myofibroblastic tumor with nuclear membrane or perinuclear ALK. American Journal of Surgical Pathology 2011;35:135–44.
[80] Panagopoulos I, Nilsson T, Domanski HA, Isaksson M, Lindblom P, Mertens F, et al. Fusion of the SEC31L1 and ALK genes in an inflammatory myofibroblastic tumor. International Journal of Cancer 2006;118:1181–6.
[81] Adam P, Katzenberger T, Seeberger H, Gattenlöhner S, Wolf J, Steinlein C, et al. A case of a diffuse large B-cell lymphoma of plasmablastic type associated with the t(2;5)(p23;q35) chromosome translocation. American Journal of Surgical Pathology 2003;27:1473–6.
[82] Onciu M, Behm FG, Downing JR, Shurtleff SA, Raimondi SC, Ma Z, et al. ALK-positive plasmablastic B-cell lymphoma with expression of the NPM-ALK fusion transcript: report of 2 cases. Blood 2003;102:2642–4.
[83] De Paepe P, Baens M, van Krieken H, Verhasselt B, Stul M, Simons A, et al. ALK activation by the CLTC-ALK fusion is a recurrent event in large B-cell lymphoma. Blood 2003;102:2638–41.
[84] Takeuchi K, Soda M, Togashi Y, Ota Y, Sekiguchi Y, Hatano S, et al. Identification of a novel fusion, SQSTM1-ALK, in ALK-positive large B-cell lymphoma. Haematologica 2011;96:464–7.
[85] Bedwell C, Rowe D, Moulton D, Jones G, Bown N, Bacon CM. Cytogenetically complex SEC31A-ALK fusions are recurrent in ALK-positive large B-cell lymphomas. Haematologica 2011;96:343–6.
[86] Van Roosbroeck K, Cools J, Dierickx D, Thomas J, Vandenberghe P, Stul M, et al. ALK-positive large B-cell lymphomas with cryptic SEC31A-ALK and NPM1-ALK fusions. Haematologica 2010;95:509–13.
[87] Lin E, Li L, Guan Y, Soriano R, Rivers CS, Mohan S, et al. Exon array profiling detects EML4-ALK fusion in breast, colorectal, and non-small cell lung cancers. Molecular Cancer Research 2009;7:1466–76.
[88] Lipson D, Capelletti M, Yelensky R, Otto G, Parker A, Jarosz M, et al. Identification of new ALK and RET gene fusions from colorectal and lung cancer biopsies. Nature Medicine 2012;18:382–4.
[89] Jazii FR, Najafi Z, Malekzadeh R, Conrads TP, Ziaee AA, Abnet C, et al. Identification of squamous cell carcinoma associated proteins by proteomics and loss of beta tropomyosin expression in esophageal cancer. World Journal of Gastroenterology 2006;12:7104–12.
[90] Du XL, Hu H, Lin DC, Xia SH, Shen XM, Zhang Y, et al. Proteomic profiling of proteins dysregulated in Chinese esophageal squamous cell carcinoma. Journal of Molecular Medicine 2007;85:863–75.
[91] Debelenko LV, Raimondi SC, Daw N, Shivakumar BR, Huang D, Nelson M, et al. Renal cell carcinoma with novel VCL-ALK fusion: new representative of ALK-associated tumor spectrum. Modern Pathology 2011;24:430–42.
[92] Collins LG, Haines C, Perkel R, Enck RE. Lung cancer: diagnosis and management. American Family Physician 2007;75:56–63.
[93] Sanders HR, Li HR, Bruey JM, Scheerle JA, Meloni-Ehrig AM, Kelly JC, et al. Exon scanning by reverse transcriptase-polymerase chain reaction for detection of known and novel EML4-ALK fusion variants in non-small cell lung cancer. Cancer Genetics 2011;204:45–52.
[94] Li Y, Ye X, Liu J, Zha J, Pei L. Evaluation of EML4-ALK fusion proteins in non-small cell lung cancer using small molecule inhibitors. Neoplasia 2011;13:1–11.
[95] Sandler A, Gray R, Perry MC, Brahmer J, Schiller JH, Dowlati A, et al. Paclitaxel-carboplatin alone or with bevacizumab for non-small-cell lung cancer. New England Journal of Medicine 2006;355:2542–50.
[96] Cataldo VD, Gibbons DL, Pérez-Soler R, Quintás-Cardama A. Treatment of non-small-cell lung cancer with erlotinib or gefitinib. New England Journal of Medicine 2011;364:947–55.
[97] Lenz G, Staudt LM. Aggressive lymphomas. New England Journal of Medicine 2010;362:1417–29.
[98] Cheson BD, Leonard JP. Monoclonal antibody therapy for B-cell non-Hodgkin's lymphoma. New England Journal of Medicine 2008;359:613–26.
[99] Butrynski JE, D'Adamo DR, Hornick JL, Dal Cin P, Antonescu CR, Jhanwar SC, et al. Crizotinib in ALK-rearranged inflammatory myofibroblastic tumor. New England Journal of Medicine 2010;363:1727–33.
[100] Armstrong F, Duplantier MM, Trempat P, Hieblot C, Lamant L, Espinos E, et al. Differential effects of X-ALK fusion proteins on proliferation, transformation, and invasion properties of NIH3T3 cells. Oncogene 2004;23:6071–82.
[101] Maris JM. Recent advances in neuroblastoma. New England Journal of Medicine 2010;362:2202–11.
[102] Murugan AK, Xing M. Anaplastic thyroid cancers harbor novel oncogenic mutations of the ALK gene. Cancer Research 2011;71:4403–11.
[103] Carén H, Abel F, Kogner P, Martinsson T. High incidence of DNA mutations and gene amplifications of the ALK gene in advanced sporadic neuroblastoma tumours. Biochemical Journal 2008;416:153–9.
[104] Del Grosso F, De Mariano M, Passoni L, Luksch R, Tonini GP, Longo L. Inhibition of N-linked glycosylation impairs ALK phosphorylation and disrupts pro-survival signaling in neuroblastoma cell lines. BMC Cancer 2011;11: 525.
[105] Lerch C, Richter B. Pharmacotherapy options for advanced thyroid cancer: a systematic review. Drugs 2012;72:67–85.
[106] Nagaiah G, Hossain A, Mooney CJ, Parmentier J, Remick SC. Anaplastic thyroid cancer: a review of epidemiology, pathogenesis, and treatment. Journal of Oncology 2011;2011:542358.
[107] Neff RL, Farrar WB, Kloos RT, Burman KD. Anaplastic thyroid cancer. Endocrinology and Metabolism Clinics of North America 2008;37: 52–8.
[108] Burningham Z, Hashibe M, Spector L, Schiffman JD. The epidemiology of sarcoma. Clinical Sarcoma Research 2012;2:14.
[109] Dasgupta R, Rodeberg DA. Update on rhabdomyosarcoma. Seminars in Pediatric Surgery 2012;21:68–78.
[110] van Gaal JC, Flucke UE, Roeffen MH, de Bont ES, Sleijfer S, Mavinkurve-Groothuis AM, et al. Anaplastic lymphoma kinase aberrations in rhabdomyosarcoma: clinical and prognostic implications. Journal of Clinical Oncology 2012;30:308–15.
[111] Trusolino L, Bertotti A, Comoglio PM. MET signalling: principles and functions in development, organ regeneration and cancer. Nature Reviews Molecular Cell Biology 2010;11:834–48.

[112] Cooper CS, Park M, Blair DG, Tainsky MA, Huebner K, Croce CM, et al. Molecular cloning of a new transforming gene from a chemically transformed human cell line. Nature 1984;311:29–33.
[113] Cui JJ, Tran-Dubé M, Shen H, Nambu M, Kung PP, Pairish M, et al. Structure based drug design of crizotinib (PF-02341066), a potent and selective dual inhibitor of mesenchymal-epithelial transition factor (c-MET) kinase and anaplastic lymphoma kinase (ALK). Journal of Medicinal Chemistry 2011;54:6342–63.
[114] Eder JP, Vande Woude GF, Boerner SA, LoRusso PM. Novel therapeutic inhibitors of the c-Met signaling pathway in cancer. Clinical Cancer Research 2009;15:2207–14.
[115] Peters S, Adjei AA. MET: a promising anticancer therapeutic target. Nature Reviews Clinical Oncology 2012;9:314–26.
[116] Gherardi E, Birchmeier W, Birchmeier C, Vande Woude G. Targeting MET in cancer: rationale and progress. Nature Reviews Cancer 2012;12:89–103.
[117] Gao J, Inagaki Y, Song P, Qu X, Kokudo N, Tang W. Targeting c-Met as a promising strategy for the treatment of hepatocellular carcinoma. Pharmacological Research 2012;65:23–30.
[118] Di Renzo MF, Olivero M, Martone T, Maffe A, Maggiora P, Stefani AD, et al. Somatic mutations of the MET oncogene are selected during metastatic spread of human HNSC carcinomas. Oncogene 2000;19:1547–55.
[119] Xin X, Yang S, Ingle G, Zlot C, Rangell L, Kowalski J, et al. Hepatocyte growth factor enhances vascular endothelial growth factor-induced angiogenesis *in vitro* and *in vivo*. American Journal of Pathology 2001;158:1111–20.
[120] Roskoski Jr R. Vascular endothelial growth factor (VEGF) signaling in tumor progression. Critical Reviews in Oncology/Hematology 2007;62: 179–213.
[121] Christensen JG, Zou HY, Arango ME, Li Q, Lee JH, McDonnell SR, et al. Cytoreductive antitumor activity of PF-2341066, a novel inhibitor of anaplastic lymphoma kinase and c-Met, in experimental models of anaplastic large-cell lymphoma. Molecular Cancer Therapy 2007;6:3314–22.
[122] Kwak EL, Bang YJ, Camidge DR, Shaw AT, Solomon B, Maki RG, et al. Anaplastic lymphoma kinase inhibition in non-small-cell lung cancer. New England Journal of Medicine 2010;363:1693–703. Erratum in: New England Journal of Medicine 2011;364:588.
[123] Camidge DR, Doebele RC. Treating ALK-positive lung cancer – early successes and future challenges. Nature Reviews Clinical Oncology 2012;9: 268–77.
[124] Winer E, Gralow J, Diller L, Karlan B, Loehrer P, Pierce L, et al. Clinical cancer advances 2008: major research advances in cancer treatment, prevention, and screening – a report from the American Society of Clinical Oncology. Journal of Clinical Oncology 2009;27:812–26. Erratum in: Journal of Clinical Oncology 2009;27:3070–1.
[125] Katayama R, Shaw AT, Khan TM, Mino-Kenudson M, Solomon BJ, Halmos B, et al. Mechanisms of acquired crizotinib resistance in ALK-rearranged lung Cancers. Science Translational Medicine 2012;4:120ra17.
[126] Sasaki T, Okuda K, Zheng W, Butrynski J, Capelletti M, Wang L, et al. The neuroblastoma-associated F1174L ALK mutation causes resistance to an ALK kinase inhibitor in ALK-translocated cancers. Cancer Research 2010;70:10038–43.
[127] Choi YL, Soda M, Yamashita Y, Ueno T, Takashima J, Nakajima T, et al. EML4-ALK mutations in lung cancer that confer resistance to ALK inhibitors. New England Journal of Medicine 2010;363:1734–9.
[128] Zuccotto F, Ardini E, Casale E, Angiolini M. Through the gatekeeper door: exploiting the active kinase conformation. Journal of Medicinal Chemistry 2010;53:2681–94.
[129] Azam M, Seeliger MA, Gray NS, Kuriyan J, Daley GQ. Activation of tyrosine kinases by mutation of the gatekeeper threonine. Nature Structural & Molecular Biology 2008;15:1109–18.
[130] Lovly CM, Heuckmann JM, de Stanchina E, Chen H, Thomas RK, Liang C, et al. Insights into ALK-driven cancers revealed through development of novel ALK tyrosine kinase inhibitors. Cancer Research 2011;71:4920–31.
[131] Lovly CM, Pao W. Escaping ALK inhibition: mechanisms of and strategies to overcome resistance. Science Translational Medicine 2012;4(120): 120ps2.
[132] Sasaki T, Koivunen J, Ogino A, Yanagita M, Nikiforow S, Zheng W, et al. A novel ALK secondary mutation and EGFR signaling cause resistance to ALK kinase inhibitors. Cancer Research 2011;71:6051–60.
[133] Doebele RC, Pilling AB, Aisner DL, Kutateladze TG, Le AT, Weickhardt AJ, et al. Mechanisms of resistance to crizotinib in patients with ALK gene rearranged non-small cell lung cancer. Clinical Cancer Research 2012;18: 1472–82.
[134] Heuckmann JM, Hölzel M, Sos ML, Heynck S, Balke-Want H, Koker M, et al. ALK mutations conferring differential resistance to structurally diverse ALK inhibitors. Clinical Cancer Research 2011;17:7394–401.
[135] Katayama R, Khan TM, Benes C, Lifshits E, Ebi H, Rivera VM, et al. Therapeutic strategies to overcome crizotinib resistance in non-small cell lung cancers harboring the fusion oncogene EML4-ALK. Proceedings of the National Academy of Sciences of the United States of America 2011;108: 7535–40.
[136] Roskoski Jr R. STI-571: an anticancer protein-tyrosine kinase inhibitor. Biochemical Biophysical Research Communications 2003;309:709–17.
[137] Kinoshita K, Asoh K, Furuichi N, Ito T, Kawada H, Hara S, et al. Design and synthesis of a highly selective, orally active and potent anaplastic lymphoma kinase inhibitor (CH5424802). Bioorganic and Medicinal Chemistry 2012;20:1271–80.
[138] Sakamoto H, Tsukaguchi T, Hiroshima S, Kodama T, Kobayashi T, Fukami TA, et al. CH5424802, a selective ALK inhibitor capable of blocking the resistant gatekeeper mutant. Cancer Cell 2011;19:679–90.
[139] Kinoshita K, Kobayashi T, Asoh K, Furuichi N, Ito T, Kawada H, et al. 9-Substituted 6,6-dimethyl-11-oxo-6,11-dihydro-5H-benzo[b]carbazoles as highly selective and potent anaplastic lymphoma kinase inhibitors. Journal of Medicinal Chemistry 2011;54:6286–94.
[140] Kuromitsu S, Mori M, Shimada I, Kondoh Y, Shindoh N, Soga T, et al. Antitumor activities of ASP3026 against EML4-ALK-dependent tumor models. Molecular Cancer Therapeutics 2011;10(11 Suppl.). Abstract A227.
[141] Sabbatini P, Korenchuk S, Rowand JL, Groy A, Liu Q, Leperi D, et al. GSK1838705A inhibits the insulin-like growth factor-1 receptor and anaplastic lymphoma kinase and shows antitumor activity in experimental models of human cancers. Molecular Cancer Therapeutics 2009;8:2811–20.
[142] Cheng M, Quail MR, Gingrich DE, Ott GR, Lu L, Wan W, et al. CEP-28122, a highly potent and selective orally active inhibitor of anaplastic lymphoma kinase with antitumor activity in experimental models of human cancers. Molecular Cancer Therapy 2012;11:67–9.
[143] Gingrich DE, Lisko JG, Curry MA, Cheng M, Quail M, Lu L, et al. Discovery of an orally efficacious inhibitor of anaplastic lymphoma kinase. Journal of Medicinal Chemistry 2012;55:4580–93.
[144] Ott GR, Wells GJ, Thieu TV, Quail MR, Lisko JG, Mesaros EF, et al. 2,7-Disubstituted-pyrrolo[2,1-f][1,2,4]triazines: new variant of an old template and application to the discovery of anaplastic lymphoma kinase (ALK) inhibitors with in vivo antitumor activity. Journal of Medicinal Chemistry 2011;54:6328–41.
[145] Lewis RT, Bode CM, Choquette DM, Potashman M, Romero K, Stellwagen JC, et al. The discovery and optimization of a novel class of potent, selective, and orally bioavailable anaplastic lymphoma kinase (ALK) inhibitors with potential utility for the treatment of cancer. Journal of Medicinal Chemistry 2012;55:6523–40.
[146] Lipinski CA, Lombardo F, Dominy BW, Feeney PJ. Experimental and computational approaches to estimate solubility and permeability in drug discovery and development settings. Advanced Drug Delivery Reviews 1997;23: 3–25.
[147] Smith GF. Medicinal chemistry by the numbers: the physicochemistry, thermodynamics and kinetics of modern drug design. Progress in Medicinal Chemistry 2009;48:1–29.
[148] Leeson PD, Springthorpe B. The influence of drug-like concepts on decision-making in medicinal chemistry. Nature Reviews Drug Discovery 2007;6:881–90.
[149] Rowley JD. Letter: a new consistent chromosomal abnormality in chronic myelogenous leukaemia identified by quinacrine fluorescence and Giemsa staining. Nature 1973;243:290–3.
[150] Groffen J, Stephenson JR, Heisterkamp N, de Klein A, Bartram CR, Grosveld G. Philadelphia chromosomal breakpoints are clustered within a limited region, bcr, on chromosome 22. Cell 1984;36:93–9.
[151] Khorashad JS, Deininger MW. Selection of therapy: rational decisions based on molecular events. Hematology/Oncology Clinics of North America 2011;25:1009–23.
[152] Hughes TP, Hochhaus A, Branford S, Müller MC, Kaeda JS, Foroni L, et al. Long-term prognostic significance of early molecular response to imatinib in newly diagnosed chronic myeloid leukemia: an analysis from the International Randomized Study of Interferon and STI571 (IRIS). Blood 2010;116: 3758–65.
[153] Kantarjian H, Sawyers C, Hochhaus A, Guilhot F, Schiffer C, Gambacorti-Passerini C, et al. Hematologic and cytogenetic responses to imatinib mesylate in chronic myelogenous leukemia. New England Journal of Medicine 2002;346:645–52. Erratum in: New England Journal of Medicine 2002;346:1923.
[154] Jabbour E, Parikh SA, Kantarjian H, Cortes J. Chronic myeloid leukemia: mechanisms of resistance and treatment. Hematology/Oncology Clinics of North America 2011;25:981–95.
[155] Ohanian M, Cortes J, Kantarjian H, Jabbour E. Tyrosine kinase inhibitors in acute and chronic leukemias. Expert Opinion on Pharmacotherapy 2012;13:927–38.
[156] Roskoski Jr R. The ErbB/HER receptor protein-tyrosine kinases and cancer. Biochemical and Biophysical Research Communications 2004;319: 1–11.
[157] Ghosh G, Lian X, Kron SJ, Palecek SP. Properties of resistant cells generated from lung cancer cell lines treated with EGFR inhibitors. BMC Cancer 2012;12:95.
[158] Pao W, Miller VA, Politi KA, Riely GJ, Somwar R, Zakowski MF, et al. Acquired resistance of lung adenocarcinomas to gefitinib or erlotinib is associated with a second mutation in the EGFR kinase domain. PLoS Medicine 2005;2(3): e73.
[159] Yun CH, Mengwasser KE, Toms AV, Woo MS, Greulich H, Wong KK, et al. The T790M mutation in EGFR kinase causes drug resistance by increasing the affinity for ATP. Proceedings of the National Academy of Sciences of the United States of America 2008;105:2070–5.
[160] Flaherty KT, Puzanov I, Kim KB, Ribas A, McArthur GA, Sosman JA, et al. Inhibition of mutated, activated BRAF in metastatic melanoma. New England Journal of Medicine 2010;363:809–19.
[161] Tuma RS. Getting around PLX4032: studies turn up unusual mechanisms of resistance to melanoma drug. Journal of the National Cancer Institute 2011;103:170–7.

[162] Zou HY, Li Q, Lee JH, Arango ME, McDonnell SR, Yamazaki S, et al. An orally available small-molecule inhibitor of c-Met, PF-2341066, exhibits cytoreductive antitumor efficacy through antiproliferative and antiangiogenic mechanisms. Cancer Research 2007;67:4408–17.
[163] Gerber DE, Minna JD. ALK inhibition for non-small cell lung cancer: from discovery to therapy in record time. Cancer Cell 2010;18:548–51.
[164] Druker BJ, Lydon NB. Lessons learned from the development of an abl tyrosine kinase inhibitor for chronic myelogenous leukemia. Journal of Clinical Investigation 2000;105:3–7.
[165] Roskoski Jr R. RAF protein-serine/threonine kinases: structure and regulation. Biochemical Biophysical Research Communications 2010;399:313–7.